NOAA Technical Memorandum ERL SEL-45

ATS-6 NOAA SOLID STATE PROTON EXPERIMENT:
MEAN ENERGY OF A FINITE ENERGY PASSBAND

J. A. McKinnon
T. A. Fritz

Space Environment Laboratory
Boulder, Colorado
December 1976

NATIONAL OCEANIC AND ATMOSPHERIC ADMINISTRATION / Environmental Research Laboratories

DEFINITIONS OF PRINCIPAL SYMBOLS

For additional definitions see section 7, a summary of the analytical and numerical solutions developed in this document.

ATS-6	Sixth in the series of Applications Technology Satellites; launched 30 May 1974 into synchronous orbit
SSPD	Solid State Proton Detector; a silicon slab with electrical contacts on each surface
ΔE	Low energy passband identifying label designating the highest discriminator level tripped; $\Delta E3$, for example implies threshold 3 and not 4 has been triggered and that the incident particle's energy lies between these two levels; table 9 lists the approximate energy range associated with each "bin" into which the experiment package assigns incoming charged particles
ΔH	High energy passband identifying label; remarks above for the ΔE channels apply.
E_n and E_{n+1}	Low- and high-side "limits" of an energy passband that denote incident particle energies for which electronic discrimination levels are 50% efficient
$\phi_n(E)$ and $\phi_{n+1}(E)$	Front- and back-side cumulative distribution functions of a gaussian curve
$\xi_n(E)$	Passband efficiency function formed as the difference between $\phi_n(E)$ and $\phi_{n+1}(E)$
FWHM	Full width at half the maximum of a normal probability density function; measures the total system noise
$\varepsilon_n^{\pm}$ and $\varepsilon_{n+1}^{\pm}$	Integration limits removed 3 FWHM above and below the lower and upper 50% transmission energies
σ_n and σ_{n+1}	Standard deviations, i.e., measures of the width, of the normal probability density functions associated with an energy passband's low- and high-sides
$\Phi(x)$	Cumulative distribution function of the *standardized* gaussian curve; a standardized probability function is centered about zero along the x axis, has an argument expressed in standard deviation units or z scores and, when integrated over all x, equals unity

(Continued Inside Back Cover)

NOAA Technical Memorandum ERL SEL-45

ATS-6 NOAA SOLID STATE PROTON EXPERIMENT: MEAN ENERGY OF A FINITE ENERGY PASSBAND

J. A. McKinnon
T. A. Fritz

Space Environment Laboratory
Boulder, Colorado
December 1976

UNITED STATES
DEPARTMENT OF COMMERCE
Elliot L. Richardson, Secretary

NATIONAL OCEANIC AND
ATMOSPHERIC ADMINISTRATION
Robert M. White, Administrator

Environmental Research
Laboratories
Wilmot N. Hess, Director

JOHN ANGUS MCKINNON

Mr. McKinnon was born in El Paso, Texas, on August 4, 1941. He received the B.S. degree in physics from the University of Texas at El Paso in 1963 and the M.S. degree in astrogeophysics from the University of Colorado in 1966. As a member of the Space Environment Laboratory since 1967, he has helped to assemble quantitative historiographies of major solar activity and their diverse terrestrial effects, participated in the development of several solar geomagnetic warning techniques, and served on radiation hazard teams in support of the Apollo manned lunar missions. His present activities include an investigation of magnetospherically trapped heavy ions near the geomagnetic equator and enrollment in an advanced degree program in mathematical archaeology.

THEODORE A. FRITZ

Dr. Fritz was born in Kingsport, Tennessee, on June 25, 1939. He received the B.S. degree in physics from Virginia Polytechnic Institute in 1961 and the M.S. and Ph.D. degrees in physics from the University of Iowa in 1964 and 1967. He worked on the design, construction, and calibration of many scientific experiments for satellite programs before coming to the NOAA Space Environment Laboratory in 1971. He is involved in the NASA/TIROS-N space environment monitoring definition and is co-investigator on experiments to be flown on the NASA/ISEE A and B spacecraft which will be launched in the fall of 1977. During 1973, he was a visiting scientist in residence at the Max Planck Institute for Aeronomy in Lindau/Harz, Germany.

CONTENTS

Page

ABSTRACT 1

1. INTRODUCTION 1

2. DETECTOR EFFICIENCY FUNCTION 2

3. MEAN ENERGY EXPRESSION 4

4. EVALUATION OF DETECTOR RESPONSE 5

5. EVALUATION OF MEAN ENERGY 10

6. NUMERICAL INTEGRATIONS 13

7. SUMMARY OF RESULTS 16

8. APPLICATION TO THE ATS-6 NOAA LOW ENERGY PROTON EXPERIMENT 18

9. VERIFICATION OF RESULTS 39

10. ACKNOWLEDGMENTS 39

11. BIBLIOGRAPHY 41

APPENDIX A: DEFINITION OF THE FWHM 42

FIGURES

1. Detector efficiency of a hypothetical passband as a function of incident particle energy. 3

2. Relationship between efficiency and the full width at half maximum for the lower discriminator level of a hypothetical passband. 20

3. ATS-6 low and high energy SSPD response ratios of adjacent passbands as a function of positive spectral parameter values. 33

4. ATS-6 low and high energy SSPD response ratios of adjacent passbands as a function of negative spectral parameter values. 34

5. Mean energies of the ATS-6 low and high energy SSPD passbands as a function of positive spectral parameter values. 35

Page

6. Mean energies of the ATS-6 low and high energy SSPD passbands as a function of negative spectral parameter values. 36

7. ATS-6 low energy SSPD responses in keV units as a function of spectral parameter. 37

8. ATS-6 high energy SSPD responses in keV units as a function of spectral parameter. 38

9. Differential energy proton spectrum. 40

A.1 Definition of the full width at half maximum (FWHM) for the gaussian or normal probability density function. 43

TABLES

1. Evaluation of ideal detector efficiency function. 4

2. Limits of detector responses, response ratios, and mean energies of selected ATS-6 NOAA experiment passbands. 19

3. Positive spectral parameter evaluation of ATS-6 low and high energy SSPD response ratios. 21

4. Negative spectral parameter evaluation of ATS-6 low and high energy SSPD response ratios. 23

5. Positive spectral parameter evaluation of mean energies in keV units for the ATS-6 SSPD passbands. 25

6. Negative spectral parameter evaluation of mean energies in keV units for the ATS-6 SSPD passbands. 27

7. ATS-6 low energy SSPD responses in keV units as a function of spectral parameter. 29

8. ATS-6 high energy SSPD responses in keV units as a function of spectral parameter. 31

ATS-6 NOAA SOLID STATE PROTON EXPERIMENT:

MEAN ENERGY OF A FINITE ENERGY PASSBAND

J. A. McKinnon and T. A. Fritz

Mathematically the observed counting rate of a particle telescope is the integral over all positive energies of the product of the geometric factor, the passband efficiency as a function of incident particle energy, and the form of the sampled particle spectrum. Using the difference of two gaussian integrals to generate the measured detector efficiency profile and an experimentally verified form of the proton differential energy spectrum, predicted counting rates for selected channels of the ATS-6 NOAA Low Energy Proton Experiment have been computed, tabulated and graphed for a wide range of anticipated proton spectra slopes. Tables and graphs presented as a function of particle spectrum slope for each passband include not only the theoretical detector response but counting rate ratios of adjacent energy windows and the spectrum-slope-weighted mean energies, $\langle E \rangle$. From these three quantities proton spectra consisting of (x,y) coordinate pairs of the form $[\langle E \rangle, j_0 \exp(-\langle E \rangle/E_0)]$ are constructed from observed counting rates to yield a profile more accurately reflecting the trend of the underlying particle spectrum.

1. INTRODUCTION

Have you ever viewed a sports event through a picket fence with closely spaced, wide upright stakes? An accurate interpretation of activities behind the fence depends, short of climbing over it, on the width of the wooden pales and their separation. Although the analogy may be incomplete, reconstructing the true particle spectrum from a set of electronic discriminator levels, that in turn form the logic circuit of a satellite-borne solid state proton detector (SSPD), poses similar limitations in resolving detail. Plotting counts per second against energy for a coarse family of adjoining energy channels not only smoothes over the true spectrum's profile but highlights a second problem: *Where does one plot the observed counting rate within a wide window when contributions to the measured counting rate are not uniformly distributed across the channel*? Ideally the representative point to be plotted for each passband is the weighted mean energy, since it is this quantity that will properly reflect the changing emphasis in the counting rate within each window's limits. This report outlines the theory necessary to determine the approximate true weighted mean of an energy passband, and thereby isolate the funtional dependence of the mean energy on the particle spectrum slope.

The somewhat tedious integrations that follow are presented with few algebraic steps omitted in order to encourage future application of these general expressions to similar detector instrumentation. An exponential form of the differential energy spectrum is assumed, characterized by a multiplicative constant j_0 and a quantity E_0 proportional to the spectrum's slope. Expressions for the detector response, the response ratio, and the mean energy are derived for any particle passband of arbitrary but finite width as a function of the differential energy spectrum's slope parameter E_0. Furthermore, through the development important analytical expressions have been highlighted by framing.

2. DETECTOR EFFICIENCY FUNCTION

Initially one must consider an energy passband with lower and upper limits that are generated using electronic discriminator levels—thresholds labeled here as E_n and E_{n+1}. These low- and high-side limits have been equated with those energies at which particle detection is 50% efficient. Although the selection is a convenient one, a choice must nevertheless be made, as electronically the two edges of the window are not infinitely sharp. For solid state detectors with electronically determined passbands, the leading edge, the window itself, and the backside portions of the efficiency function may be reproduced mathematically using an integral fundamental to statistics: the cumulative distribution function of the familiar normal distribution. The complete response is generated as the difference of two cumulative distribution functions, one representing the frontside of the passband and another the backside (see fig. 1). These two expressions adapted to a window of arbitrary width are reproduced below.

$$\text{Frontside cumulative distribution function} = \frac{1}{\sqrt{2\pi}\,\sigma_n} \int_{-\infty}^{E} \exp[-(E'-E_n)^2/2\sigma_n{}^2]\, dE' = \phi_n(E)$$

$$\text{Backside cumulative distribution function} = \frac{1}{\sqrt{2\pi}\,\sigma_{n+1}} \int_{-\infty}^{E} \exp[-(E''-E_{n+1})^2/2\sigma_{n+1}^2]\, dE'' = \phi_{n+1}(E)$$

$$\text{Detector efficiency over entire window} = \xi_n(E) = \phi_n(E) - \phi_{n+1}(E)$$

To illustrate that $\xi_n(E)$ does indeed give the intended response, it is evaluated for the critical energies marked in figure 1 and summarized in table 1. Before this calculation may be completed, however, it is necessary to define an energy sufficiently removed from the 50% value to insure that the integral of the normal distribution function is effectively zero or

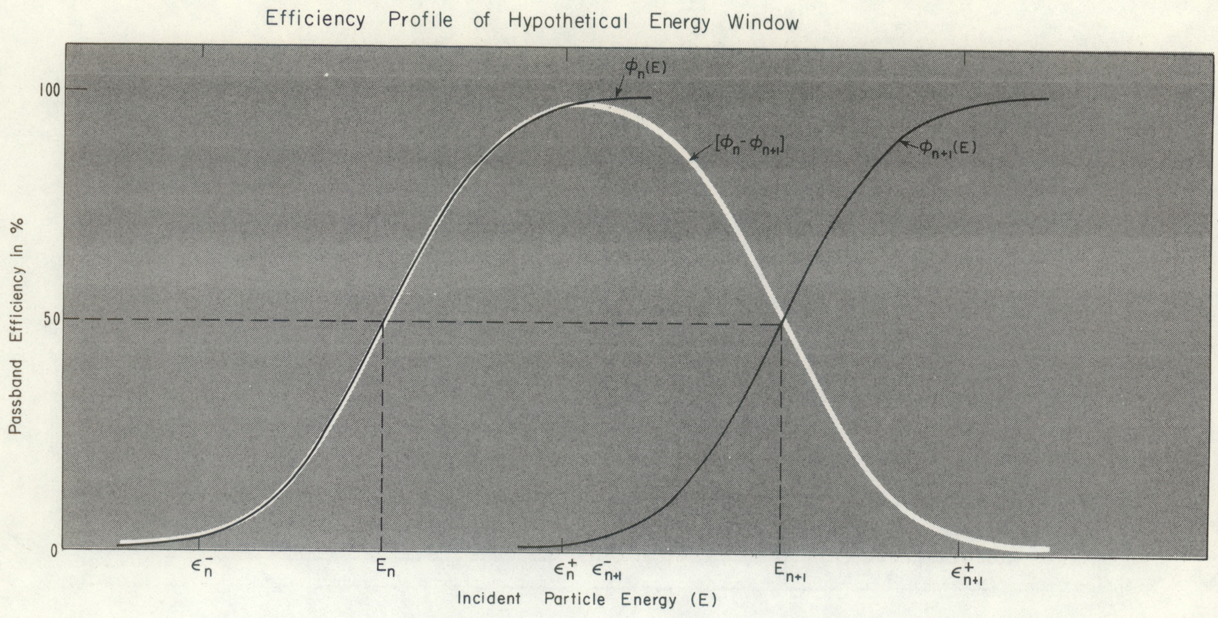

Figure 1. Detector efficiency of hypothetical passband as a function of incident particle energy (white curve). The curve represents the difference between the two step-like functions, $\phi_n(E)$ and $\phi_{n+1}(E)$ shown in solid black line. Note the energies E_n and E_{n+1} are used to label the limits of the window illustrated above even though the instrument is sensitive to particles with energies above and below these values. Some choice as to where a passband's discriminator levels should be arises, for noise within the system produces less-than-infinitely-sharp edges. These levels are commonly set equal to the 50% transmission energies, points designated here as E_n and E_{n+1}. The epsilons along the x axis mark integration limits defined in the text.

unity. These values of the incident particle energy have been chosen to lie $3(2\sigma\sqrt{2\ell n2})$ or three full width half maxima (FWHM) to either side of E_n and E_{n+1} and are marked along the x axis of figure 1 but not to scale. Later in the development these same energies, which are defined below, serve as limits in the numerical solution offered as an alternative.

$$\varepsilon_n^{\pm} = E_n \pm 3\text{FWHM} = E_n \pm 3(2\sigma_n\sqrt{2\ell n2})$$

$$\varepsilon_{n+1}^{\pm} = E_{n+1} \pm 3\text{FWHM} = E_{n+1} \pm 3(2\sigma_{n+1}\sqrt{2\ell n2})$$

The term FWHM is defined and discussed in Appendix A.

Table 1. Evaluation of Ideal Detector Efficiency Function $\xi_n(E)$

E	$\phi_n(E)$	$\phi_{n+1}(E)$	$\phi_n(E)-\phi_{n+1}(E)$
$<<E_n$	0	0	0
ε_n^-	0	0	0
E_n	0.5	0	0.5
ε_n^+	1	0	1
ε_{n+1}^-	1	0	1
E_{n+1}	1	0.5	0.5
ε_{n+1}^+	1	1	0
$>>E_{n+1}$	1	1	0

3. MEAN ENERGY EXPRESSION

Computing the mean energy of an arbitrary passband between discriminator levels E_n and E_{n+1} necessitates evaluating the weighted mean of E with respect to the weighting function $[g\xi_n(E)j_0 \exp(-E/E_0)]$

where g = the telescope's geometric factor in units of cm^2 ster
$\xi_n(E)$ = the passband efficiency function
$j_0\exp(-E/E_0)$ = an experimentally verified form of the differential energy spectrum in units of protons/cm^2 sec ster keV.

Despite the algebraically complex weighting function given above, the mean value of E is, at least in principle, a straightforward computation. Furthermore, E's mean value is insured because of the weighting function's continuity, that is, because it has a unique slope at each point on its profile. After writing the integral of E and its weighting function over the passband interval as an identity, one simply asks for what value of the energy may it be removed from within the integral sign. This value, denoted here as <E> represents the properly weighted mean of E, and its solution as outlined below is seen to be a quotient of integrals.

$$\int_0^\infty E\,[g\xi_n(E)j_0 \exp(-E/E_0)]dE = \int_0^\infty E\,[g\xi_n(E)j_0 \exp(-E/E_0)]dE$$

$$\langle E\rangle \int_0^\infty g\xi_n(E)j_o \exp(-E/E_o)dE = \int_0^\infty E[g\xi_n(E)j_0 \exp(-E/E_0)]dE$$

$\langle E \rangle$ above has been relabeled $\langle E_{n,n+1} \rangle$ throughout the remainder of the paper in order to emphasize the particular particle energy window to which the mean of E refers. The mean energy of a passband with 50% transmission energies E_n and E_{n+1} sampling an exponential differential energy spectrum is expressed in its most complete form by the ratio

$$\langle E_{n,n+1} \rangle = \left\{ \int_0^\infty E[g\xi_n(E)j_0 \exp(-E/E_0)]dE \right\} \Big/ \int_0^\infty g\xi_n(E)j_0 \exp(-E/E_0)dE .$$

An evaluation of $\langle E_{n,n+1} \rangle$ follows in which it is convenient to consider the integral in the denominator separately, for this expression represents the detector response function. In the next section the response function's complicated form is reduced in detail to the algebraic sum of several cumulative distribution functions.

4. EVALUATION OF DETECTOR RESPONSE

$$\text{Detector Response} = R_{n,n+1} = \int_0^\infty g\xi_n(E)j_0 \exp(-E/E_0)dE$$

$$= \int_0^\infty g[\phi_n(E) - \phi_{n+1}(E)]j_0 \exp(-E/E_0)dE$$

where $\phi_n(E)$ and $\phi_{n+1}(E)$ are the integrals defined in section 2. For ease of reference the involved expression representing $R_{n,n+1}$ is split into two integrals of identical form and designated I_1 and I_2. Thus $R_{n,n+1} = gj_0(I_1 - I_2)$.

$$\text{where } I_1 = \int_0^\infty \phi_n(E) \exp(-E/E_0)dE = \int_0^\infty \left\{ C_n \int_{-\infty}^{E} \exp[-(E'-E_n)^2/2\sigma_n{}^2]dE' \right\} \exp(-E/E_0)dE$$

$$\text{and } I_2 = \int_0^\infty \phi_{n+1}(E) \exp(-E/E_0)\, dE$$

$$= \int_0^\infty \left\{ C_{n+1} \int_{-\infty}^{E} \exp[-(E''-E_{n+1})^2/2\sigma^2_{n+1}]\, dE'' \right\} \exp(-E/E_0)\, dE .$$

In the above equations $C_n = 1/\sqrt{2\pi}\ \sigma_n$ and $C_{n+1} = 1/\sqrt{2\pi}\ \sigma_{n+1}$.

In the following development the technique of integration by parts has been applied to I_1. Fortunately, the integrand's form leaves little choice as to how it should be subdivided, and the assignment is

$$u = C_n \int_{-\infty}^{E} \exp[(-E'-E_n)^2/2\sigma_n^2] \cdot dE' \text{ and } dv = \exp(-E/E_0)\ dE.$$

To complete the preliminary computations the technique requires u to be differentiated and dv integrated, both with respect to E. Moreover, the legitimacy of differentiating within the integral sign is upheld under the circumstances since the integrand of u is a continuous function over the range of integration. These two operations yield

$$\frac{du}{dE} = C_n \exp[-(E-E_n)^2/2\sigma_n^2] \quad \text{and } v = -\ E_0 \exp(-E/E_0)\ .$$

Completing the integration by parts yields the following:

$$I_1 = \int_0^\infty udv = uv \Big|_0^\infty - \int_0^\infty vdu$$

$$= \left[\left(C_n \int_{-\infty}^{E} e^{-(E'-E_n)^2/2\sigma_n^2}\ dE'\right)\left(-E_0 e^{-E/E_0}\right)\right]_0^\infty$$

$$- \int_0^\infty -E_0 e^{-E/E_0}\ C_n e^{-(E-E_n)^2/2\sigma_n^2}\ dE\ .$$

This expression reduces to

$$I_1 = E_0C_n \int_{-\infty}^{0} \exp[-(E'-E_n)^2/2\sigma_n^2]\, dE' + E_0C_n \int_{0}^{\infty} \exp(-E/E_0)\, \exp[-(E-E_n)^2/2\sigma_n^2] dE\ .$$

Before I_1 may be completely evaluated the power to which e is raised in the second integral must be rewritten as a perfect square.

Thus we have $-E/E_0 - (E-E_n)^2/2\sigma_n^2$ taking the form $-\beta_n/2\sigma_n^2 - (E+\alpha_n)^2/2\sigma_n{}^2$

if one sets $\alpha_n = \sigma_n^2/E_0 - E_n$ and $\beta_n = E_n^2 - \alpha_n^2$. (A number of lines of algebra have been omitted here.) I_1 is then rewritten as

$$I_1 = E_0C \int_{\infty}^{0} \exp[-(E'-E_n)^2/2\sigma_n^2]\, dE' + E_0 \exp(-\beta_n/2\sigma_n^2)\, C_n \int_{0}^{\infty} \exp[-(E+\alpha_n)^2/2\sigma_n^2\, dE].$$

Now if we let $s = (E'-E_n)/\sigma_n$ and $t = (E+\alpha_n)/\sqrt{2}\,\sigma_n$

then $ds = dE'/\sigma_n$ and $dt = dE/\sqrt{2}\,\sigma_n$

and the integrals constituting I_1 may be cast into either of two forms: (1) that of the cumulative distribution function of the *standardized* normal probability density function or (2) the complementary error function. The definitions of these integral expressions are reproduced below.

Cumulative distribution function $= \Phi(x) = \dfrac{1}{\sqrt{2\pi}} \displaystyle\int_{-\infty}^{x} e^{-s^2/2}\, ds$

Complementary error function $= \mathrm{erfc}(y) = \dfrac{2}{\sqrt{\pi}} \displaystyle\int_{y}^{\infty} e^{-t^2} dt$

Making use of the substitutions s and t indicated above and the definitions of Φ and erfc, I_1 is transformed into

$$I_1 = E_0 C_n \int_{-\infty}^{-E_n/\sigma_n} e^{-s^2/2} \sigma_n ds + E_0 e^{-\beta_n/2\sigma_n^2} C_n \int_{\alpha_n/\sqrt{2}\,\sigma_n}^{\infty} e^{-t^2} \sqrt{2}\, \sigma_n \, dt$$

and then

$$I_1 = \frac{E_0}{\sqrt{2\pi}\,\sigma_n} \sigma_n \sqrt{2\pi}\, \Phi(-E_n/\sigma_n) + \frac{E_0\sqrt{2}}{\sqrt{2\pi}\sigma_n} \sigma_n \cdot \frac{\sqrt{\pi}}{2} \operatorname{erfc}(\alpha_n/\sqrt{2}\,\sigma_n)\, e^{-\beta_n/2\sigma_n^2} . \qquad (1)$$

If it is recognized that the cumulative distribution functions are related, then equation (1) may be further simplified by expressing it solely in terms of either Φ or erfc. The necessary relationship between these two functions is derived in the following four lines.

$$\Phi(x) = \frac{1}{\sqrt{2\pi}} \int_{-\infty}^{x} e^{-s^2/2} ds = \frac{1}{\sqrt{2\pi}} \int_{-\infty}^{x/\sqrt{2}} e^{-t^2} \sqrt{2}\, dt \text{ if we let } t = s/\sqrt{2} .$$

$$\Phi(x) = \frac{1}{\sqrt{2\pi}} \int_{-\infty}^{0} e^{-t^2} \sqrt{2}\, dt + \frac{1}{\sqrt{2\pi}} \int_{0}^{x/\sqrt{2}} e^{-t^2} \sqrt{2}\, dt$$

$$= \frac{\sqrt{2}}{\sqrt{2\pi}} \cdot \frac{\sqrt{\pi}}{2} + \frac{\sqrt{2}}{\sqrt{2\pi}} \cdot \frac{\sqrt{\pi}}{2} \operatorname{erf}(x/\sqrt{2})$$

$$\Phi(x) = \tfrac{1}{2} + \tfrac{1}{2} [1 - \operatorname{erfc}(x/\sqrt{2})] = 1 - \tfrac{1}{2} \operatorname{erfc}(x/\sqrt{2})$$

$$\operatorname{erfc}(x/\sqrt{2}) = 2[1 - \Phi(x)] = 2\Phi(-x) \qquad (2)$$

Substituting the result of equation (2) into (1) casts I_1 into its final and most elegant form shown below.

$$\boxed{I_1 = E_0\ \Phi(-E_n/\sigma_n) + E_0\ \Phi(-\alpha_n/\sigma_n)\ \exp\ (-\beta_n/2\sigma_n^2)}$$

Because I_2, defined along with I_1 in the previous section, is identical in form to I_1, its integral may be written as

$$\boxed{I_2 = E_0\ \Phi(-E_{n+1}/\sigma_{n+1}) + E_0\ \Phi(-\alpha_{n+1}/\sigma_{n+1})\ \exp(-\beta_{n+1}/2\sigma_{n+1}^2)\quad .}$$

Having completed the integrations of both I_1 and I_2, the final expression for the detector response in units of counts/sec may be written. This quantity, which characterizes a window between the discriminator levels E_n and E_{n+1} is seen to be a function of the standard deviations σ_n and σ_{n+1}, the slope of the differential energy spectrum E_0, and, of course, the window's lower and upper limits, E_n and E_{n+1}. As defined on page 5, $R_{n,n+1} = g\ j_0(I_1 - I_2)$. Therefore differencing these two integrals yields

$$R_{n,n+1}(\text{counts/sec}) = g\ j_0E_0\Big\{\Phi(-E_n/\sigma_n) + \Phi(-\alpha_n/\sigma_n)\ \exp(-\beta_n/2\sigma_n^2)$$

$$- \Phi(-E_{n+1}/\sigma_{n+1}) - \Phi(-\alpha_{n+1}/\sigma_{n+1})\ \exp(-\beta_{n+1}/2\sigma_{n+1}^2)\Big\}. \qquad (3)$$

Since the ratio of the responses of two energy passbands determines the slope of the differential energy spectrum, it is important to consider experimentally this quotient. Once equation (3) is evaluated passband by passband for a wide range of E_0, the ratio of adjacent windows as a function of this same parameter is easily determined. It then becomes possible to identify quickly a slope for a given detector response ratio by means of the table so generated. Although the technique is a straightforward one, should the particle spectrum be characterized by a slope that is a strong function of energy, the passbands must be closely spaced in order to trace its complicated profile. The general relation for the ratio of adjacent windows is defined here as the quotient of lower energy window to higher:

$$r_{n,n+1} = R_{n,n+1}/R_{n+1,n+2}\ .$$

5. EVALUATION OF MEAN ENERGY

Up to this point only the denominator in the mean energy expression discussed in section 3 has been evaluated. Using the definition of the detector response function, the relation for $\langle E_{n,n+1} \rangle$ is rewritten below to emphasize the remaining portion.

$$\langle E_{n,n+1} \rangle = \left\{ \int_0^\infty E[g\xi_n(E) j_0 \exp(-E/E_0)]dE \right\} / R_{n,n+1}$$

Since the integral in the above equation itself contains integrals, subsequent mathematical manipulations are more easily followed if several of the terms are grouped and redefined. One such partition is given below.

$$R_{n,n+1} \langle E_{n,n+1} \rangle = \int_0^\infty E[g\xi_n(E) j_0 \exp(-E/E_0)]dE = \int_0^\infty E\Big\{ g[\phi_n(E)$$

$$- \phi_{n+1}(E)]\ j_0 \exp(-E/E_0) \Big\}\ dE \ .$$

$$\frac{R_{n,n+1}}{gj_0} \langle E_{n,n+1} \rangle = \int_0^\infty E \left\{ C_n \int_{-\infty}^{E} \exp[-(E'-E_n)^2/2\sigma_n^2]\ dE' \right.$$

$$\left. -C_{n+1} \int_{\infty}^{E} \exp[-(E''-E_{n+1})^2/2\sigma_{n+1}^2] dE'' \right\} \exp(-E/E_0)\ dE = I_3 - I_4 \ .$$

Once again the technique of integration by parts is appealed to. Here the integrand of I_3 is subdivided into the two components shown below—a choice no less restrictive than before. Thus

$$I_3 = \int_0^\infty E \left\{ C_n \int_{-\infty}^{E} \exp[-(E'-E_n)^2/2\sigma_n^2] dE' \right\} \exp(-E/E_0) dE$$

and $\quad u = EC_n \displaystyle\int_{-\infty}^{E} \exp[-(E'-E_n)^2/2\sigma_n^2]\ dE'$ and $dv = \exp(-E/E_0)\ dE$.

One also needs

$$\frac{du}{dE} = C_n \int_{-\infty}^{E} \exp[-(E'-E_n)^2/2\sigma_n^2]\, dE' + EC_n \exp[-(E-E_n)^2/2\sigma_n^2]$$

$$\text{and } v = -E_0 \exp(-E/E_0) \, .$$

These four quantities are then combined according to the technique's prescription (see section 4) to yield

$$I_3 = \left\{ EC_n \int_{-\infty}^{E} \exp\,[-(E'-E_n)^2/2\sigma_n^2]\, dE' \right\} [-E_0 \exp(-E/E_0)] \Bigg|_0^{\infty}$$

$$- \int_0^{\infty} [-E_0 \exp(-E/E_0)] \left\{ C_n \int_{-\infty}^{E} \exp\,[-(E'-E_n)^2/2\sigma_n^2]\, dE' \right.$$

$$\left. + EC_n \exp\,[-(E-E_n)^2/2\sigma_n^2] \right\} dE. \qquad (4)$$

At the upper limit the first term in equation (4) is of the form ∞/∞, allowing L'Hospital's rule to be applied in the evaluation of the function's limit.

$$\text{Thus } \lim_{E\to\infty} \left[\frac{-E\phi_n(E)E_0}{\exp(E/E_0)} \right] = \lim_{E\to\infty} \left\{ \frac{-\phi_n(E)E_0 - EC_n \exp[-(E-E_n)^2/2\sigma_n^2]\, E_0}{\exp(E/E_0)/E_0} \right\}.$$

A second application of L'Hospital's rule is required to justify setting the above limit equal to zero. Finally, this same first term in equation (4) vanishes at the lower limit, and in what remains of I_3, the leading integral is identical to I_1 defined earlier aside from the multiplicative constant E_0. These simplifications reduce I_3 to the following form:

$$I_3 = E_0 I_1 + E_0 C_n \int_0^\infty E \exp(-E/E_0) \exp[-(E-E_n)^2/2\sigma_n^2] \, dE \, .$$

Once again the expression representing the power to which e is raised is converted to a perfect square. Consequently I_3 takes on the following form:

$$I_3 = E_0 I_1 + E_0 C_n \exp(-\beta_n/2\sigma_n^2) \int_0^\infty E \exp[-(E + \alpha_n)^2/2\sigma_n^2] \, dE \, .$$

A change of variables then allows the remaining integral to be expressed in terms of the by now familiar cumulative distribution and error functions. The required substitutions follow.

Let $t = (E+\alpha_n)/\sqrt{2}\,\sigma_n$; then $dt = dE/\sqrt{2}\,\sigma_n$ and $E = \sqrt{2}\,\sigma_n t - \alpha_n$.

Then I_3 becomes

$$I_3 = E_0 I_1 + E_0 C_n e^{-\beta_n/2\sigma_n^2} \int_{\alpha_n/\sqrt{2}\sigma_n}^{\infty} (\sqrt{2}\,\sigma_n t - \alpha_n) e^{-t^2} \sqrt{2}\,\alpha_n \, dt \, .$$

The first term within the integrand may be integrated explicitly, and with some rearranging I_3 takes the form

$$I_3 = E_0 I_1 + E_0 C_n e^{-\beta_n/2\sigma_n^2} \sqrt{2}\,\sigma_n \left\{ \sqrt{2}\,\sigma_n \left[-\frac{e^{-t^2}}{2} \right]_{\alpha_n/\sqrt{2}\,\sigma_n}^{\infty} - \alpha_n \int_{\alpha_n/\sqrt{2}\,\sigma_n}^{\infty} e^{-t^2} dt \right\} .$$

The two final steps invoke the definition of the complementary error function and its relation to the cumulative distribution function given in equation (2).

$$I_3 = E_0 I_1 + E_0 \frac{\sqrt{2}\,\sigma_n}{\sqrt{2\pi}\,\sigma_n} e^{-\beta_n/2\sigma_n^2} \left[\frac{\sqrt{2}}{2} \sigma_n e^{-\alpha_n^2/2\sigma_n^2} - \alpha_n \frac{\sqrt{\pi}}{2} \operatorname{erfc}(\alpha_n/\sqrt{2}\,\sigma_n) \right]$$

$$\boxed{I_3 = E_0 I_1 + \frac{E_0}{\sqrt{\pi}} e^{-\beta_n/2\sigma_n^2} \left[\frac{\sigma_n}{\sqrt{2}} e^{-\alpha_n^2/2\sigma_n^2} - \alpha_n \sqrt{\pi}\; \Phi(-\alpha_n/\sigma_n) \right]}$$

The integral expression labeled I_4 has an algebraic form identical to I_3 in which n is replaced by n+1.

6. NUMERICAL INTEGRATIONS

The principal advantage of the algebraic approach outlined in the previous sections lies in its minuscule computing cost. These relatively complex solutions for the detector response, response ratio and mean energy may be evaluated and graphed quickly and inexpensively on a programmable calculator. On the other hand, a numerical integration of the functions is straightforward conceptually, but it can involve several hundred dollars in computing charges. The numerical procedure is presented here as an alternative technique because it allows the investigator (1) to modify easily the functional form used in representing the differential energy spectrum, (2) to compare results with those from the derived equations, and (3) to generate look-up tables.

Care must be exercised in numerically evaluating an integral of the form illustrated by $R_{n,n+1}$. If computed in its entirety rather than partitioned into the segments labeled earlier as I_1 and I_2, much inconvenience may be eliminated, for the integrands of I_1 and other expressions of that ilk approach zero slowly as E_0 itself assumes small values. The order in which the terms are evaluated is critical because the product of a unit step function and an exponential containing a negative argument does not cut off rapidly for extreme values of the variable. Thus the integration range must be greatly extended beyond the convenient interval of zero to ε_{n+1}^{+} in order to obtain a particular degree of precision. However, the complete integrand of $R_{n,n+1}$ does isolate a small energy range over which the function differs from zero, and a series of 1000 terms or more generates converging results agreeing with the expressions derived for $R_{n,n+1}$ and $\langle E_{n,n+1} \rangle$ to five significant figures.

The trapezoidal rule is applied below to approximate the complicated expressions (I_1 - I_2) and (I_3 - I_4), resulting in a finite series, each term of which includes the difference of two cumulative distribution functions. It remains then to evaluate these integrals. Here one may apply any of several approximations to the integral of the standardized gaussian function, depending on the range of the independent variable and the desired precision. (See equations 6 and 7 on the next page.)

The numerical solution to the detector response function is given below. Note that a simple change of variables converts the lower case phis (the cumulative distribution function) to upper case phis (the integral of the standardized gaussian function).

$$(I_1 - I_2) = R_{n,n+1}/gj_0 = \int_0^{\infty} [\phi_n(E) - \phi_{n+1}(E)] \exp(-E/E_0)\, dE$$

$$\cong \int_0^{\varepsilon_{n+1}^{+}} \left\{\Phi[(E-E_n)/\sigma_n] - \Phi[(E-E_{n+1})/\sigma_{n+1}]\right\} \exp(-E/E_0)\, dE$$

$$\cong \Delta E \left\{\tfrac{1}{2}[\Phi(x_0) - \Phi(y_0)]\, e^{-z_0} + [\Phi(x_1) - \Phi(y_1)]\, e^{-z_1}\right.$$

$$\left. + \cdots + \tfrac{1}{2}\left[\Phi(x_N) - \Phi(y_N)\right] e^{-z_N} \right\} \tag{5}$$

where $x_i = (E_i-E_n)\alpha_n$

$y_i = (E_i-E_{n+1})/\sigma_{n+1}$

$z_i = E_i/E_0$

$E_i = i\Delta E$

$\Delta E = (E_{n+1} + 3\mathrm{FWHM})/N = [E_{n+1} + 3(2\sqrt{2\ell n 2}\ \sigma_{n+1})]/N$

One of the following two relations has been used to evaluate the standardized gaussian function denoted here as Φ. (See section 7 for the numerical values of the constants C_1 through C_5 and p.)

$$\Phi(s) \cong 1 - \exp(-s^2/2)(C_1t + C_2t^2 + \cdots + C_5t^5)/\sqrt{2\pi} \quad \text{for } 0 \le s \le \propto \tag{6}$$

$$\Phi(s) \cong \exp(-s^2/2)(C_1t + C_2t^2 + \cdots + C_5t^5)/\sqrt{2\pi} \quad \text{for } s < 0 \tag{7}$$

where $t = 1/[1 + p|s|]$

In a similar manner one may evaluate $(I_3 - I_4)$, the integral expression proportional to the product of the weighted mean energy and detector response. Note $(I_3 - I_4)$ differs from $(I_1 - I_2)$ only in the presence of the multiplicative factor E.

$$(I_3 - I_4)/gj_0 = \langle E_{n,n+1} \rangle (R_{n,n+1}/gj_0) = \int_0^\infty E[\phi_n(E) - \phi_{n+1}(E)] \exp(-E/E_0)\, dE$$

$$\cong \int_0^{\varepsilon_{n+1}^+} E\{\Phi[(E-E_n)/\sigma_n] - \Phi[(E-E_{n+1})/\sigma_{n+1}]\} \exp(-E/E_0)\, dE$$

$$\cong \Delta E \left\{ \frac{w_0}{2} [\Phi(x_0) - \Phi(y_0)]\, e^{-z_0} + w_1[\Phi(x_1) - \Phi(y_1)]\, e^{-z_1} \right.$$

$$\left. + \cdots + \frac{w_N}{2} [\Phi(x_N) - \Phi(y_N)]\, e^{-z_N} \right\} \qquad (8)$$

In equation (8) w_i has been used to replace E_i to minimize any confusion that might arise between E_0, the spectral parameter, and the value of E_i when $i = 0$. The quantities x_i, y_i and z_i are identical to the definitions following equation (5).

7. SUMMARY OF RESULTS

7.1 Analytic Solution*

Detector Response = $R_{n,n+1} = gj_0(I_1 - I_2)$

Response Ratio of Adjacent Passbands = $r_{n,n+1} = R_{n,n+1}/R_{n+1,n+2}$

Mean Energy = $\langle E_{n,n+1} \rangle = gj_0(I_3 - I_4)/R_{n,n+1} = (I_3 - I_4)/(I_1 - I_2)$

Assumed form of the differential energy spectrum: $j = j_0 \exp(-E/E_0)$

where $I_1 = E_0\, \Phi(-E_n/\sigma_n) + E_0\, \Phi(-\alpha_n/\sigma_n) \exp(-\beta_n/2\sigma_n^2)$

I_2 is identical in form to I_1 with n replaced by n+1.

$$I_3 = E_0 I_1 + \frac{E_0}{\sqrt{\pi}} \exp\left(-\beta_n/2\sigma_n^2\right) \left[(\sigma_n/\sqrt{2}) \exp(-\alpha_n^2/2\sigma_n^2) - \alpha_n \sqrt{\pi}\, \Phi(-\alpha_n/\sigma_n)\right]$$

and I_4 is identical in form to I_3 with n replaced by n+1.

Definitions of the quantities used in I_1 through I_4:

$\alpha_n = \sigma_n^2/E_0 - E_n$ $\qquad$ $\alpha_{n+1} = \sigma_{n+1}^2/E_0 - E_{n+1}$

$\beta_n = E_n^2 - \alpha_n^2$ $\qquad$ $\beta_{n+1} = E_{n+1}^2 - \alpha_{n+1}^2$

$\sigma_n = (\text{FWHM})_n / 2\sqrt{2\ell n 2}$ $\qquad$ $\sigma_{n+1} = (\text{FWHM})_{n+1} / 2\sqrt{2\ell n 2}$

$\Phi(x)$ = cumulative distribution function = $\frac{1}{\sqrt{2\pi}} \int_{-\infty}^{x} \exp(-s^2/2)ds$

$\Phi(x)$ is approximated by the finite series indicated below.

$\Phi(x) \cong 1 - \exp(-x^2/2)(C_1 t + C_2 t^2 + \cdots + C_5 t^5)/\sqrt{2\pi}$ for $0 \le x \le \infty$

$\phi(x) \cong \exp(-x^2/2)(C_1 t + C_2 t^2 + \cdots + C_5 t^5)\ \sqrt{2\pi}$ for $x < 0$

where $t = 1/[1 + p|x|]$

$C_1 = 0.319381530$

$C_2 = -\ 0.356563782$

$C_3 = 1.781477937$

$C_4 = -1.821255978$

$C_5 = 1.330274429$

$p = 0.2316419$

*The hierarchy of equations tabulated in either column should help to clarify the ultimate dependencies of the detector responses, response ratios, and mean energies on assumed and experimentally measured quantities, namely E_0, E_n, $(\text{FWHM})_n$, E_{n+1} and $(\text{FWHM})_{n+1}$.

7.2 Numerical Solution*

Detector Response = $R_{n,n+1} = gj_0(I_1-I_2)$

Response Ratio of Adjacent Passbands = $r_{n,n+1} = R_{n,n+1}/R_{n+1,n+2}$

Mean Energy = $\langle E_{n,n+1}\rangle = gj_0(I_3-I_4)/R_{n,n+1} = (I_3-I_4)/(I_1-I_2)$

Assumed form of the differential energy spectrum: $j = j_0 \exp(-E/E_0)$

where $$(I_1-I_2) \cong \Delta E \{\tfrac{1}{2}[\Phi(x_0) - \Phi(y_0)]e^{-z_0} + [\Phi(x_1) - \Phi(y_1)]e^{-z_1} + [\Phi(x_2) - \Phi(y_2)]e^{-z_2} + \cdots + \tfrac{1}{2}[\Phi(x_N) - \Phi(y_N)]e^{-z_N}\}$$

and $$(I_3-I_4) \cong \Delta E \left\{\frac{w_0}{2} [\Phi(x_0) - \Phi(y_0)]e^{-z_0} + w_i [\Phi(x_1) - \Phi(y_1)]e^{-z_1} + w_2[\Phi(x_2) - \Phi(y_2)]e^{-z_2} + \cdots + \frac{w_N}{2} [\Phi(x_N) - \Phi(y_N)]e^{-z_N}\right\}$$

One thousand terms were used in each of the above finite series approximations.

Definitions of the quantities used in (I_1-I_2) and (I_3-I_4):

$x_i = (E_i-E_n)/\sigma_n$; $y_i = (E_i-E_{n+1})/\sigma_{n+1}$; $z_i = E_i/E_0$; $w_i = E_i$

The limits of integration along the incident energy axis for the lower and upper discriminator levels are

$\varepsilon_n^{\pm} = E_n \pm 3(2\sqrt{2\ell n2}\ \sigma_n)$ and $\varepsilon_{n+1}^{\pm} = E_{n+1} \pm 3(2\sqrt{2\ell n2}\ \sigma_{n+1})$.

$\Delta E = [E_{n+1} + 3(2\sqrt{2\ell n2}\ \sigma_{n+1})]/N$; $E_i = i\Delta E$

$\sigma_n = (\mathrm{FWHM})_n/ 2\sqrt{2\ell n2}$; $\sigma_{n+1} = (\mathrm{FWHM})_{n+1}/ 2\sqrt{2\ell n2}$

$\Phi(x)$ = cumulative distribution function = $\dfrac{1}{\sqrt{2\pi}} \displaystyle\int_{-\infty}^{x} \exp(-s^2/2)ds$

$\Phi(x)$ is approximated by the finite series indicated below.

$\Phi(x) \cong 1 - \exp(-x^2/2)(C_1t + C_2t^2 + \cdots + C_5t^5)/\sqrt{2\pi}$ for $0 \le x \le \infty$

$\phi(x) \cong \exp(-x^2/2)(C_1t + C_2t^2 + \cdots + C_5t^5)/\sqrt{2\pi}$ for $x < 0$

where $t = 1/[1 + p|x|]$

$C_1 = 0.319381530$

$C_2 = -0.356563782$

$C_3 = 1.781477937$

$C_4 = -1.821255978$

$C_5 = 1.330274429$

$p = 0.2316419$

8. APPLICATION TO THE ATS-6 NOAA LOW ENERGY PROTON EXPERIMENT

The numerical solution summarized in section 7 has been applied to selected passbands of the NOAA Low Energy Proton Experiment carried on board ATS-6. For details of this package see Fritz and Cessna (1975).

The lower and upper 50% electronic discriminator levels in keV units for selected channels of the ATS-6 proton experiment package are listed in table 2 under the column headings E_n and E_{n+1}. These values along with an average FWHM were determined from experimentally measured detector efficiency profiles using the particle acceleration facilities of NASA/GSFC. An example of such a profile is presented in figure 2.

The detector response and mean energy for each passband, and the detector response ratio of adjacent windows, are evaluated numerically over a range of E_0 and presented in tables 3-8 and graphed in figures 3-8. When used in the manner outlined below, the tables provide a quick estimate of the corrected or properly weighted mean energy for each proton channel.

1) Compute the response ratio of adjacent energy windows from the experimentally measured total counting rate within each passband.

2) Using the ratio of a particular passband pair and tables 3 and 4, determine E_0, a quantity proportional to the slope of the spectrum between the two energy channels.

3) With E_0 and tables 5 and 6 estimate the true weighted mean value of the window's energy.

4) Compute the multiplicative constant j_0 by dividing the observed counting rate by the product of the geometric factor and the theoretically evaluated detector response listed in tables 7 and 8.

5) Combine E_0 and j_0 with the mean energy and compute the approximate differential flux, $j_0 \exp(-\langle E\rangle/E_0)$.

Finally in order to reconstruct the slope-corrected particle spectrum, the mean energy and differential flux associated with each passband are treated as a new (x,y) coordinate pair, replacing points on the spectrum's profile composed of the arithmetic mean of E_n and E_{n+1} and the observed flux.

Table 2. Limits of Detector Responses, Response Ratios, and Mean Energies of Selected ATS-6 NOAA Experiment Passbands.

Passband	Frontside E_n (keV)	Frontside $(FWHM)_n$ (keV)	Backside E_{n+1} (keV)	Backside $(FWHM)_{n+1}$ (keV)	$\ell im\ (R/gj_0)$ (keV)	$\ell im\ r_{n,n+1}$	Arithmetic Mean (keV)	$\ell im\ \langle E_{n,n+1}\rangle$** (keV)
Low Energy Solid State Detectors (B Telescope)								
ΔE1	25.5	9.37	33.4	9.37	7.9000	0.54861	29.450	29.450
ΔE2	33.4	9.37	47.8	9.37	14.400	0.62609	40.600	40.600
ΔE3	47.8	9.37	70.8	9.37	23.000	0.78231	59.300	59.300
ΔE4	70.8	9.37	100.2	9.37	29.400	0.58450	85.500	85.500
ΔE5	100.2	9.37	150.5	9.37	50.299	0.60240	125.35	125.35
ΔE6	150.5	9.37	234	9.37	83.498		192.25	192.25
ΔE7	234	9.37	2800	9.37	2565.6		1517.0	1516.9
D2L2	3660	9.37	$4E_0\ell n10$*	9.37	9953.0E3			
High Energy Solid State Detectors (H Telescope)								
ΔH1	374.9	33.6	384	25	9.0997	0.47895	379.45	374.46
ΔH2	386.9	30.5	405.9	27.3	18.999	0.39338	396.40	395.52
ΔH3	408.2	26.6	456.5	33.3	48.298	0.67364	432.35	433.10
ΔH4	456.5	33.3	528.2	29.5	71.696	0.51178	492.35	492.05
ΔH5	532.2	30.2	672.3	28.4	140.09	0.59975	602.25	602.18
ΔH6	676.7	30	910.3	26.8	233.58	1.2586	793.50	793.43
ΔH7	914.4	29.2	1100	60	185.58		1007.2	1008.5
H1P	183	60	1100	60	916.94		641.5	641.49

*For energies greater than 10^3 keV the observed differential energy spectrum $j_0 \exp(-E/E_0)$ declines sharply with increasing energy and effectively delimits a semi-infinite window. The upper limit of the D2L2 channel has been determined by that value of E satisfying the condition $j_0/10^4 = j_0 \exp(-E/E_0)$.

**For $\ell im\ \langle E_{n,n+1}\rangle$, whenever the slopes of the window's leading and following edges are not symmetric, the mean energy will not reduce to the average of the front and backside discriminator levels for a flat differential energy spectrum.

Note: Limiting values shown were computed using a flat differential energy spectrum, one in which the spectral slope parameter, E_0, was set equal to 10^7 keV. Energies specifying each channel have been extracted from experimentally measured detector efficiency profiles using the NASA/GSFC particle accelerator.

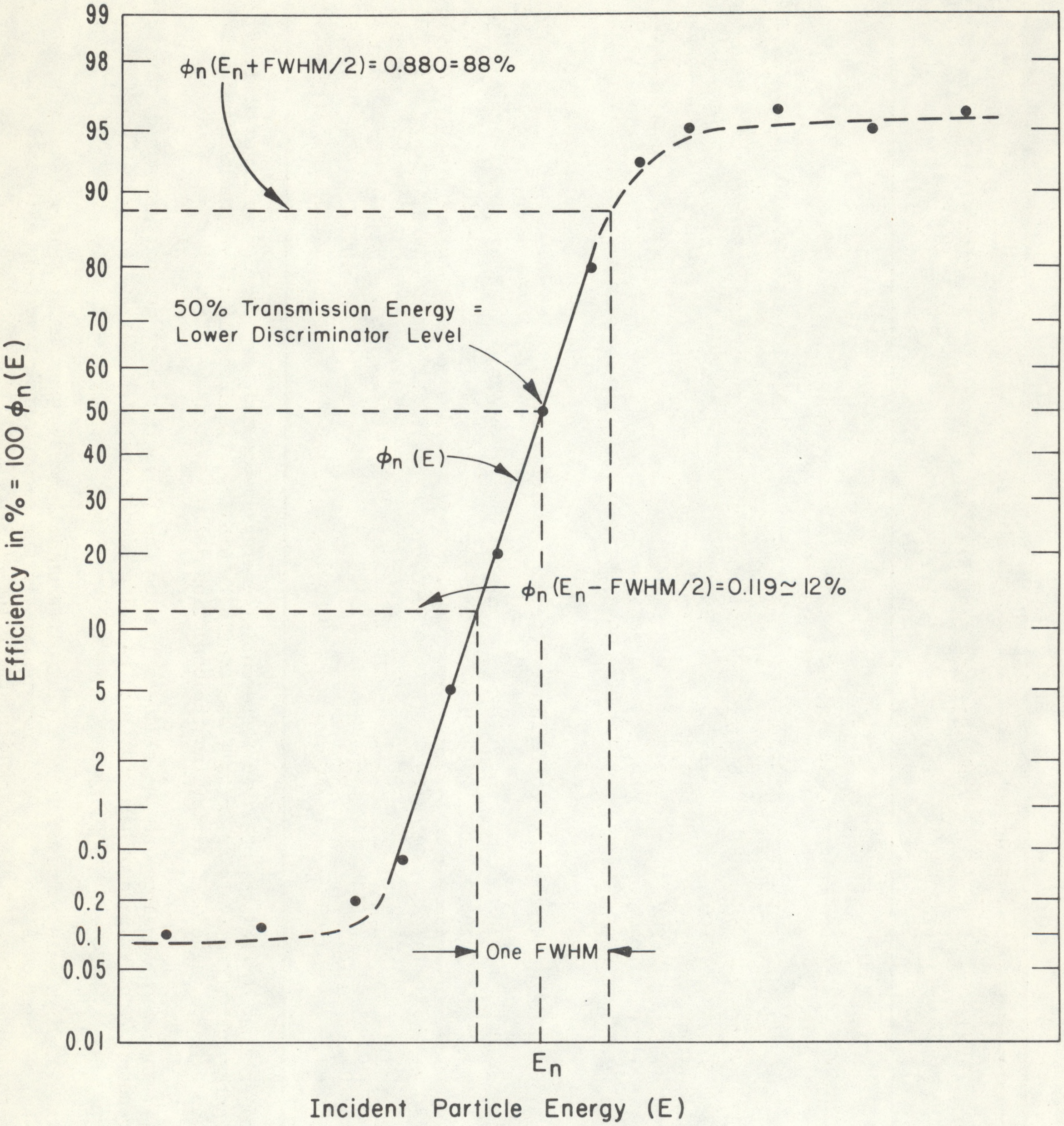

Figure 2. Relationship between efficiency and the full width at half maximum for the lower discriminator level of a hypothetical passband. Experimental points deviate from the gaussian straight-line approximation because a non-ideal monitor channel was used and the not-quite-monoenergetic particle beam was slightly contaminated with some species other than protons.

Table 3. Positive Spectral Parameter Evaluation of ATS-6 Low and High Energy SSPD Response Ratios.

E_0	$\Delta E1/\Delta E2$	$\Delta E2/\Delta E3$	$\Delta E3/\Delta E4$	$\Delta E4/\Delta E5$	E_0	$\Delta E5/\Delta E6$	$\Delta E6/\Delta E7$*	$\Delta E7/D2L2$*
1.0	2.6844E+03	1.7941E+06	9.7448E+09	5.8649E+12	1.0	6.9986E+21	0.	0.
1.5	1.9278E+02	1.4764E+04	4.5623E+06	3.2522E+08	1.5	3.6588E+14	0.	0.
2.0	5.0973E+01	1.3384E+03	9.8715E+04	2.4217E+06	2.0	8.3658E+10	0.	0.
2.5	2.2642E+01	3.1638E+02	9.8962E+03	1.2803E+05	2.5	5.4702E+08	0.	0.
3.0	1.3027E+01	1.2057E+02	2.1351E+03	1.8033E+04	3.0	1.9128E+07	0.	0.
3.5	8.6979E+00	6.0293E+01	7.1355E+02	4.4461E+03	3.5	1.7435E+06	0.	0.
4.0	6.3810E+00	3.5712E+01	3.1339E+02	1.5552E+03	4.0	2.8924E+05	0.	0.
4.5	4.9901E+00	2.3675E+01	1.6509E+02	6.8670E+02	4.5	7.1522E+04	0.	0.
5.0	4.0842E+00	1.6985E+01	9.8760E+01	3.5682E+02	5.0	2.3387E+04	0.	0.
5.5	3.4576E+00	1.2908E+01	6.4794E+01	2.0868E+02	5.5	9.3707E+03	0.	0.
6.0	3.0034E+00	1.0245E+01	4.5556E+01	1.3332E+02	6.0	4.3726E+03	0.	0.
6.5	2.6621E+00	8.4093E+00	3.3781E+01	9.1158E+01	6.5	2.2939E+03	0.	0.
7.0	2.3977E+00	7.0888E+00	2.6120E+01	6.5736E+01	7.0	1.3194E+03	0.	0.
7.5	2.1880E+00	6.1053E+00	2.0885E+01	4.9461E+01	7.5	8.1685E+02	0.	0.
8.0	2.0181E+00	5.3516E+00	1.7160E+01	3.8520E+01	8.0	5.3682E+02	0.	0.
8.5	1.8782E+00	4.7599E+00	1.4421E+01	3.0863E+01	8.5	3.7056E+02	0.	0.
9.0	1.7611E+00	4.2858E+00	1.2349E+01	2.5318E+01	9.0	2.6646E+02	0.	0.
9.5	1.6620E+00	3.8994E+00	1.0744E+01	2.1138E+01	9.5	1.9832E+02	0.	0.
10.0	1.5770E+00	3.5795E+00	9.4751E+00	1.8034E+01	10.0	1.5197E+02	0.	0.
15.0	1.1234E+00	2.0553E+00	4.2293E+00	6.3203E+00	15.0	2.7704E+01	0.	0.
20.0	9.4376E-01	1.5430E+00	2.8026E+00	3.6439E+00	20.0	1.1544E+01	0.	0.
25.0	8.4875E-01	1.2950E+00	2.1827E+00	2.5874E+00	25.0	6.7163E+00	0.	0.
30.0	7.9026E-01	1.1506E+00	1.8450E+00	2.0473E+00	30.0	4.6342E+00	0.	0.
35.0	7.5073E-01	1.0567E+00	1.6352E+00	1.7266E+00	35.0	3.5338E+00	0.	0.
40.0	7.2225E-01	9.3093E-01	1.4931E+00	1.5168E+00	40.0	2.8728E+00	0.	0.
45.0	7.0078E-01	9.4242E-01	1.3908E+00	1.3699E+00	45.0	2.4395E+00	0.	0.
50.0	6.8401E-01	9.0519E-01	1.3138E+00	1.2618E+00	50.0	2.1369E+00	0.	0.
55.0	6.7057E-01	8.7574E-01	1.2539E+00	1.1792E+00	55.0	1.9153E+00	0.	0.
60.0	6.5954E-01	8.5187E-01	1.2060E+00	1.1141E+00	60.0	1.7469E+00	0.	0.
65.0	6.5034E-01	8.3215E-01	1.1668E+00	1.0616E+00	65.0	1.6151E+00	0.	0.
70.0	6.4255E-01	8.1558E-01	1.1342E+00	1.0184E+00	70.0	1.5094E+00	0.	0.
75.0	6.3586E-01	8.0147E-01	1.1067E+00	9.8221E-01	75.0	1.4229E+00	0.	0.
80.0	6.3006E-01	[illegible].8930E-01	1.0831E+00	9.5153E-01	80.0	1.3510E+00	0.	0.
85.0	6.2499E-01	7.7871E-01	1.0627E+00	9.2519E-01	85.0	1.2903E+00	0.	0.
90.0	6.2050E-01	7.6940E-01	1.0449E+00	9.0233E-01	90.0	1.2385E+00	0.	0.
95.0	6.1652E-01	7.6116E-01	1.0292E+00	8.8232E-01	95.0	1.1937E+00	0.	0.
100.0	6.1295E-01	7.5382E-01	1.0152E+00	8.6465E-01	100.0	1.1546E+00	0.	0.
150.0	5.9079E-01	7.0879E-01	9.3104E-01	7.6001E-01	150.0	9.3329E-01	0.	0.
200.0	5.7998E-01	6.8722E-01	8.9150E-01	7.1213E-01	200.0	8.3781E-01	0.	0.
250.0	5.7358E-01	6.7457E-01	8.6856E-01	6.8474E-01	250.0	7.8490E-01	0.	0.
300.0	5.6935E-01	6.6626E-01	8.5357E-01	6.6701E-01	300.0	7.5134E-01	0.	0.
350.0	5.6634E-01	6.6038E-01	8.4303E-01	6.5461E-01	350.0	7.2818E-01	0.	0.
400.0	5.6410E-01	6.5600E-01	8.3520E-01	6.4544E-01	400.0	7.1124E-01	0.	0.
450.0	5.6236E-01	6.5261E-01	8.2916E-01	6.3840E-01	450.0	6.9831E-01	0.	0.
500.0	5.6097E-01	6.4991E-01	8.2435E-01	6.3281E-01	500.0	6.8813E-01	0.	0.
550.0	5.5984E-01	6.4771E-01	8.2044E-01	6.2827E-01	550.0	6.7989E-01	0.	0.
600.0	5.5889E-01	6.4588E-01	8.1720E-01	6.2451E-01	600.0	6.7310E-01	0.	0.
650.0	5.5810E-01	6.4434E-01	8.1446E-01	6.2135E-01	650.0	6.6741E-01	0.	0.
700.0	5.5741E-01	6.4302E-01	8.1213E-01	6.1865E-01	700.0	6.6256E-01	0.	0.
750.0	5.5682E-01	6.4188E-01	8.1010E-01	6.1631E-01	750.0	6.5838E-01	0.	0.
800.0	5.5631E-01	6.4088E-01	8.0834E-01	6.1428E-01	800.0	6.5475E-01	0.	0.
850.0	5.5585E-01	6.4000E-01	8.0679E-01	6.1249E-01	850.0	6.5156E-01	0.	0.
900.0	5.5545E-01	6.3922E-01	8.0541E-01	6.1090E-01	900.0	6.4873E-01	0.	0.
950.0	5.5508E-01	6.3852E-01	8.0418E-01	6.0949E-01	950.0	6.4621E-01	0.	0.
1000.0	5.5476E-01	6.3790E-01	8.0307E-01	6.0821E-01	1000.0	6.4395E-01	0.	0.

Table 3 (Continued)

E_0	ΔH1/ΔH2	ΔH2/ΔH3	ΔH3/ΔH4	ΔH4/ΔH5	E_0	ΔH5/ΔH6	ΔH6/ΔH7	ΔH7/H1P*
1.0	9.9157E+12	9.4419E+17	1.7919E+05	3.8729E+40	1.0	1.6875E+63	0.	0.
1.5	8.6008E+06	1.1034E+10	9.9056E+06	2.2141E+25	1.5	1.1135E+42	4.4247E+69	0.
2.0	3.5645E+04	6.4006E+06	3.6106E+06	2.3230E+18	2.0	3.1311E+31	1.2016E+52	0.
2.5	2.1383E+03	1.2469E+05	7.5032E+05	2.4223E+14	2.5	1.5055E+25	3.8864E+41	0.
3.0	3.9993E+02	1.1285E+04	1.7601E+05	6.5375E+11	3.0	9.3522E+20	4.1372E+34	0.
3.5	1.3306E+02	2.2619E+03	5.1302E+04	1.0533E+10	3.5	9.3036E+17	4.4281E+29	0.
4.0	6.1375E+01	7.1844E+02	1.8270E+04	5.0219E+08	4.0	5.2283E+15	8.3922E+25	0.
4.5	3.4601E+01	3.0450E+02	7.6775E+03	4.8585E+07	4.5	9.3103E+13	1.0764E+23	0.
5.0	2.2234E+01	1.5633E+02	3.6855E+03	7.6486E+06	5.0	3.7151E+12	5.2547E+20	0.
5.5	1.5628E+01	9.1714E+01	1.9684E+03	1.7073E+06	5.5	2.6649E+11	6.7722E+18	0.
6.0	1.1710E+01	5.9251E+01	1.1458E+03	4.9372E+05	6.0	2.9673E+10	1.8064E+17	0.
6.5	9.2008E+00	4.1128E+01	7.1541E+02	1.7391E+05	6.5	4.6330E+09	8.4278E+15	0.
7.0	7.4945E+00	3.0159E+01	4.7313E+02	7.1433E+04	7.0	9.4341E+08	6.0989E+14	0.
7.5	6.2792E+00	2.3085E+01	3.2821E+02	3.3151E+04	7.5	2.3757E+08	6.2692E+13	0.
8.0	5.3806E+00	1.8285E+01	2.3697E+02	1.6979E+04	8.0	7.1090E+07	3.5695E+12	0.
8.5	4.6958E+00	1.4830E+01	1.7697E+02	9.4276E+03	8.5	2.4521E+07	1.4811E+12	0.
9.0	4.1604E+00	1.2405E+01	1.3603E+02	5.5970E+03	9.0	9.5205E+06	3.1124E+11	0.
9.5	3.7329E+00	1.0533E+01	1.0716E+02	3.5146E+03	9.5	4.0839E+06	7.7100E+10	0.
10.0	3.3853E+00	9.0882E+00	8.6246E+01	2.3143E+03	10.0	1.9066E+06	2.1965E+10	0.
15.0	1.8100E+00	3.5043E+00	2.0466E+01	1.6700E+02	15.0	1.5338E+04	7.7691E+06	0.
20.0	1.3138E+00	2.1268E+00	9.4708E+00	4.4864E+01	20.0	1.3759E+03	1.4666E+05	0.
25.0	1.0804E+00	1.5575E+00	5.8352E+00	2.0158E+01	25.0	3.2317E+02	1.3570E+04	0.
30.0	9.4692E-01	1.2579E+00	4.1796E+00	1.1689E+01	30.0	1.2260E+02	2.7805E+03	0.
35.0	8.6106E-01	1.0761E+00	3.2739E+00	7.8475E+00	35.0	6.1094E+01	8.9765E+02	0.
40.0	8.0144E-01	9.5540E-01	2.7167E+00	5.7805E+00	40.0	3.6077E+01	3.8515E+02	0.
45.0	7.5772E-01	8.6985E-01	2.3449E+00	4.5345E+00	45.0	2.3853E+01	1.9978E+02	0.
50.0	7.2433E-01	8.0634E-01	2.0815E+00	3.7205E+00	50.0	1.7071E+01	1.1836E+02	0.
55.0	6.9802E-01	7.5741E-01	1.8866E+00	3.1560E+00	55.0	1.2945E+01	7.7228E+01	0.
60.0	6.7676E-01	7.1864E-01	1.7370E+00	2.7461E+00	60.0	1.0253E+01	5.4172E+01	0.
65.0	6.5924E-01	6.8720E-01	1.6190E+00	2.4374E+00	65.0	8.4002E+00	4.0170E+01	0.
70.0	6.4456E-01	6.6121E-01	1.5238E+00	2.1981E+00	70.0	7.0687E+00	3.1113E+01	0.
75.0	6.3207E-01	6.3938E-01	1.4454E+00	2.0079E+00	75.0	6.0781E+00	2.4951E+01	0.
80.0	6.2133E-01	6.2080E-01	1.3799E+00	1.8538E+00	80.0	5.3196E+00	2.0581E+01	0.
85.0	6.1199E-01	6.0480E-01	1.3244E+00	1.7267E+00	85.0	4.7248E+00	1.7374E+01	0.
90.0	6.0380E-01	5.9088E-01	1.2767E+00	1.6203E+00	90.0	4.2486E+00	1.4952E+01	0.
95.0	5.9655E-01	5.7865E-01	1.2355E+00	1.5301E+00	95.0	3.8608E+00	1.3076E+01	0.
100.0	5.9010E-01	5.6785E-01	1.1994E+00	1.4528E+00	100.0	3.5400E+00	1.1594E+01	0.
150.0	5.5068E-01	5.0340E-01	9.9237E-01	1.0390E+00	150.0	2.0155E+00	5.4504E+00	0.
200.0	5.3188E-01	4.7364E-01	9.0172E-01	8.7466E-01	200.0	1.5057E+00	3.7564E+00	0.
250.0	5.2089E-01	4.5653E-01	8.5107E-01	7.8759E-01	250.0	1.2595E+00	3.0100E+00	0.
300.0	5.1367E-01	4.4543E-01	8.1877E-01	7.3395E-01	300.0	1.1165E+00	2.5987E+00	0.
350.0	5.0858E-01	4.3764E-01	7.9640E-01	6.9766E-01	350.0	1.0237E+00	2.3407E+00	0.
400.0	5.0478E-01	4.3188E-01	7.8000E-01	6.7151E-01	400.0	9.5870E-01	2.1647E+00	0.
450.0	5.0185E-01	4.2745E-01	7.6745E-01	6.5178E-01	450.0	9.1082E-01	2.0372E+00	0.
500.0	4.9952E-01	4.2393E-01	7.5756E-01	6.3638E-01	500.0	8.7411E-01	1.9408E+00	0.
550.0	4.9761E-01	4.2107E-01	7.4954E-01	6.2402E-01	550.0	8.4508E-01	1.8654E+00	0.
600.0	4.9603E-01	4.1870E-01	7.4293E-01	6.1388E-01	600.0	8.2157E-01	1.8049E+00	0.
650.0	4.9470E-01	4.1670E-01	7.3737E-01	6.0542E-01	650.0	8.0215E-01	1.7553E+00	0.
700.0	4.9356E-01	4.1499E-01	7.3264E-01	5.9825E-01	700.0	7.8584E-01	1.7139E+00	0.
750.0	4.9257E-01	4.1352E-01	7.2856E-01	5.9210E-01	750.0	7.7195E-01	1.6788E+00	0.
800.0	4.9171E-01	4.1224E-01	7.2501E-01	5.8677E-01	800.0	7.5998E-01	1.6487E+00	0.
850.0	4.9095E-01	4.1110E-01	7.2189E-01	5.8210E-01	850.0	7.4956E-01	1.6227E+00	0.
900.0	4.9028E-01	4.1010E-01	7.1913E-01	5.7797E-01	900.0	7.4041E-01	1.5998E+00	0.
950.0	4.8968E-01	4.0921E-01	7.1667E-01	5.7431E-01	950.0	7.3231E-01	1.5797E+00	0.
1000.0	4.8913E-01	4.0840E-01	7.1446E-01	5.7102E-01	1000.0	7.2509E-01	1.5618E+00	0.

* Ratio not computed because either or both windows are extremely broad relative to the lower energy passbands. Consequently, derived spectrum slopes may not be representative of the underlying particle population.

Table 4. Negative Spectral Parameter Evaluation of ATS-6 Low and High Energy SSPD Response Ratios.

E_0	ΔE1/ΔE2	ΔE2/ΔE3	ΔE3/ΔE4	ΔE4/ΔE5	E_0	ΔE5/ΔE6	ΔE6/ΔE7*	ΔE7/D2L2*
-1.0	5.5718E-07	1.0262E-10	1.7051E-13	1.4289E-22	-1.0	5.4502E-37	0.	0.
-1.5	6.7384E-05	2.1917E-07	3.0749E-09	2.7331E-15	-1.5	6.6723E-25	0.	0.
-2.0	7.3276E-04	1.0123E-05	4.1292E-07	1.1953E-11	-2.0	7.3825E-19	0.	0.
-2.5	3.0270E-03	1.0073E-04	7.8101E-06	1.8281E-09	-2.5	3.1229E-15	0.	0.
-3.0	7.7019E-03	4.6454E-04	5.5429E-05	5.2276E-08	-3.0	8.1684E-13	0.	0.
-3.5	1.4871E-02	1.3783E-03	2.2460E-04	5.7342E-07	-3.5	4.3549E-11	0.	0.
-4.0	2.4193E-02	3.1057E-03	6.4096E-04	3.4552E-06	-4.0	8.5921E-10	0.	0.
-4.5	3.5151E-02	5.8187E-03	1.4475E-03	1.3961E-05	-4.5	8.7331E-09	0.	0.
-5.0	4.7223E-02	9.5833E-03	2.7744E-03	4.2638E-05	-5.0	5.5881E-08	0.	0.
-5.5	5.9966E-02	1.4376E-02	4.7195E-03	1.0621E-04	-5.5	2.5502E-07	0.	0.
-6.0	7.3028E-02	2.0110E-02	7.3401E-03	2.2700E-04	-6.0	9.0359E-07	0.	0.
-6.5	8.6149E-02	2.6662E-02	1.0656E-02	4.3120E-04	-6.5	2.6351E-06	0.	0.
-7.0	9.9142E-02	3.3900E-02	1.4654E-02	7.4654E-04	-7.0	6.5942E-06	0.	0.
-7.5	1.1188E-01	4.1689E-02	1.9300E-02	1.1999E-03	-7.5	1.4599E-05	0.	0.
-8.0	1.2426E-01	4.9906E-02	2.4541E-02	1.8156E-03	-8.0	2.9259E-05	0.	0.
-8.5	1.3625E-01	5.8438E-02	3.0318E-02	2.6139E-03	-8.5	5.4019E-05	0.	0.
-9.0	1.4781E-01	6.7183E-02	3.6567E-02	3.6101E-03	-9.0	9.3138E-05	0.	0.
-9.5	1.5892E-01	7.6075E-02	4.3222E-02	4.8148E-03	-9.5	1.5159E-04	0.	0.
-10.0	1.6958E-01	8.5030E-02	5.0220E-02	6.2339E-03	-10.0	2.3491E-04	0.	0.
-15.0	2.5404E-01	1.6983E-01	1.2857E-01	3.1131E-02	-15.0	3.7037E-03	0.	0.
-20.0	3.0947E-01	2.3731E-01	2.0404E-01	6.7749E-02	-20.0	1.4353E-02	0.	0.
-25.0	3.4785E-01	2.9011E-01	2.6835E-01	1.0674E-01	-25.0	3.1826E-02	0.	0.
-30.0	3.7579E-01	3.3075E-01	3.2169E-01	1.4368E-01	-30.0	5.3583E-02	0.	0.
-35.0	3.9698E-01	3.6297E-01	3.6591E-01	1.7711E-01	-35.0	7.7268E-02	0.	0.
-40.0	4.1359E-01	3.8903E-01	4.0286E-01	2.0682E-01	-40.0	1.0130E-01	0.	0.
-45.0	4.2694E-01	4.1048E-01	4.3406E-01	2.3308E-01	-45.0	1.2474E-01	0.	0.
-50.0	4.3789E-01	4.2844E-01	4.6067E-01	2.5629E-01	-50.0	1.4710E-01	0.	0.
-55.0	4.4705E-01	4.4366E-01	4.8362E-01	2.7685E-01	-55.0	1.6816E-01	0.	0.
-60.0	4.5481E-01	4.5674E-01	5.0357E-01	2.9514E-01	-60.0	1.8784E-01	0.	0.
-65.0	4.6147E-01	4.6808E-01	5.2107E-01	3.1148E-01	-65.0	2.0616E-01	0.	0.
-70.0	4.6725E-01	4.7800E-01	5.3653E-01	3.2616E-01	-70.0	2.2319E-01	0.	0.
-75.0	4.7232E-01	4.8676E-01	5.5029E-01	3.3938E-01	-75.0	2.3900E-01	0.	0.
-80.0	4.7679E-01	4.9455E-01	5.6260E-01	3.5136E-01	-80.0	2.5369E-01	0.	0.
-85.0	4.8076E-01	5.0152E-01	5.7369E-01	3.6226E-01	-85.0	2.6734E-01	0.	0.
-90.0	4.8432E-01	5.0779E-01	5.8372E-01	3.7220E-01	-90.0	2.8004E-01	0.	0.
-95.0	4.8753E-01	5.1346E-01	5.9284E-01	3.8131E-01	-95.0	2.9189E-01	0.	0.
-100.0	4.9043E-01	5.1861E-01	6.0116E-01	3.8968E-01	-100.0	3.0294E-01	0.	0.
-150.0	5.0917E-01	5.5237E-01	6.5653E-01	4.4675E-01	-150.0	3.8250E-01	0.	0.
-200.0	5.1878E-01	5.7001E-01	6.8602E-01	4.7807E-01	-200.0	4.2915E-01	0.	0.
-250.0	5.2463E-01	5.8084E-01	7.0432E-01	4.9782E-01	-250.0	4.5960E-01	0.	0.
-300.0	5.2856E-01	5.8816E-01	7.1678E-01	5.1139E-01	-300.0	4.8100E-01	0.	0.
-350.0	5.3138E-01	5.9345E-01	7.2581E-01	5.2130E-01	-350.0	4.9684E-01	0.	0.
-400.0	5.3351E-01	5.9744E-01	7.3265E-01	5.2884E-01	-400.0	5.0903E-01	0.	0.
-450.0	5.3517E-01	6.0056E-01	7.3801E-01	5.3478E-01	-450.0	5.1870E-01	0.	0.
-500.0	5.3650E-01	6.0307E-01	7.4233E-01	5.3957E-01	-500.0	5.2656E-01	0.	0.
-550.0	5.3759E-01	6.0513E-01	7.4589E-01	5.4352E-01	-550.0	5.3308E-01	0.	0.
-600.0	5.3850E-01	6.0685E-01	7.4886E-01	5.4683E-01	-600.0	5.3856E-01	0.	0.
-650.0	5.3927E-01	6.0831E-01	7.5138E-01	5.4965E-01	-650.0	5.4324E-01	0.	0.
-700.0	5.3994E-01	6.0957E-01	7.5355E-01	5.5207E-01	-700.0	5.4728E-01	0.	0.
-750.0	5.4051E-01	6.1065E-01	7.5544E-01	5.5418E-01	-750.0	5.5081E-01	0.	0.
-800.0	5.4101E-01	6.1161E-01	7.5709E-01	5.5603E-01	-800.0	5.5391E-01	0.	0.
-850.0	5.4146E-01	6.1245E-01	7.5855E-01	5.5767E-01	-850.0	5.5666E-01	0.	0.
-900.0	5.4185E-01	6.1320E-01	7.5985E-01	5.5913E-01	-900.0	5.5911E-01	0.	0.
-950.0	5.4221E-01	6.1387E-01	7.6102E-01	5.6044E-01	-950.0	5.6132E-01	0.	0.
-1000.0	5.4252E-01	6.1448E-01	7.6207E-01	5.6162E-01	-1000.0	5.6331E-01	0.	0.

Table 4 (Continued)

E_0	ΔH1/ΔH2	ΔH2/ΔH3	ΔH3/ΔH4	ΔH4/ΔH5	E_0	ΔH5/ΔH6	ΔH6/ΔH7	ΔH7/H1P*
-1.0	-4.9458E-10**	2.0152E-30	5.6987E-27	3.4536E-16	-1.0	1.2707E+05	-1.7548E+72**	0.
-1.5	-4.1133E-06**	2.4943E-20	2.5095E-18	1.5100E-41	-1.5	2.6174E-62	1.3828E-02	0.
-2.0	-1.5778E-04**	4.6988E-15	3.9060E-14	2.0211E-31	-2.0	1.4376E-51	4.8451E-59	0.
-2.5	-6.4719E-04**	8.3505E-12	1.0458E-11	2.3126E-25	-2.5	1.6097E-41	7.4359E-49	0.
-3.0	-1.1902E-03**	1.2302E-09	4.5378E-10	2.6083E-21	-3.0	8.5147E-35	1.0280E-39	0.
-3.5	-1.5828E-03**	3.5614E-08	7.3437E-09	2.1042E-18	-3.5	5.6276E-30	3.7667E-33	0.
-4.0	-1.6360E-03**	4.0311E-07	6.3004E-08	3.2392E-16	-4.0	2.3749E-26	2.7923E-28	0.
-4.5	-1.1491E-03**	2.5041E-06	3.4814E-07	1.6447E-14	-4.5	1.5902E-23	1.3961E-24	0.
-5.0	2.3649E-05	1.0376E-05	1.3997E-06	3.8318E-13	-5.0	2.9237E-21	1.0361E-21	0.
-5.5	1.9501E-03	3.2307E-05	4.4392E-06	5.0575E-12	-5.5	2.0952E-19	1.9577E-19	0.
-6.0	4.6303E-03	8.1633E-05	1.1742E-05	4.3548E-11	-6.0	7.3971E-18	1.3634E-17	0.
-6.5	8.0170E-03	1.7625E-04	2.6946E-05	2.6980E-10	-6.5	1.5136E-16	4.5108E-16	0.
-7.0	1.2035E-02	3.3717E-04	5.5223E-05	1.2901E-09	-7.0	2.0164E-15	3.4621E-15	0.
-7.5	1.6598E-02	5.8633E-04	1.0327E-04	5.0125E-09	-7.5	1.9049E-14	1.0208E-13	0.
-8.0	2.1616E-02	9.4478E-04	1.7912E-04	1.6450E-08	-8.0	1.3608E-13	8.6786E-13	0.
-8.5	2.7002E-02	1.4310E-03	2.9186E-04	4.6970E-08	-8.5	7.7201E-13	5.5665E-12	0.
-9.0	3.2678E-02	2.0599E-03	4.5122E-04	1.1941E-07	-9.0	3.6143E-12	2.8366E-11	0.
-9.5	3.8574E-02	2.8423E-03	6.6720E-04	2.7529E-07	-9.5	1.4391E-11	1.1950E-10	0.
-10.0	4.4630E-02	3.7849E-03	9.4963E-04	5.8391E-07	-10.0	4.9932E-11	4.2945E-10	0.
-15.0	1.0574E-01	2.1364E-02	9.0075E-03	6.8387E-05	-15.0	1.3321E-07	1.0141E-06	0.
-20.0	1.5779E-01	4.7632E-02	2.7691E-02	7.3223E-04	-20.0	6.9206E-06	3.9683E-05	0.
-25.0	1.9902E-01	7.5473E-02	5.3935E-02	2.9924E-03	-25.0	7.4039E-05	3.3431E-04	0.
-30.0	2.3162E-01	1.0146E-01	8.3680E-02	7.5517E-03	-30.0	3.5850E-04	1.3456E-03	0.
-35.0	2.5777E-01	1.2472E-01	1.1413E-01	1.4487E-02	-35.0	1.1018E-03	3.5910E-03	0.
-40.0	2.7910E-01	1.4518E-01	1.4373E-01	2.3447E-02	-40.0	2.5470E-03	7.4500E-03	0.
-45.0	2.9677E-01	1.6313E-01	1.7171E-01	3.3924E-02	-45.0	4.6683E-03	1.3101E-02	0.
-50.0	3.1163E-01	1.7888E-01	1.9777E-01	4.5419E-02	-50.0	8.1462E-03	2.0547E-02	0.
-55.0	3.2428E-01	1.9275E-01	2.2187E-01	5.7510E-02	-55.0	1.2377E-02	2.9676E-02	0.
-60.0	3.3518E-01	2.0504E-01	2.4405E-01	6.9870E-02	-60.0	1.7494E-02	4.0305E-02	0.
-65.0	3.4466E-01	2.1597E-01	2.6445E-01	8.2257E-02	-65.0	2.3398E-02	5.2226E-02	0.
-70.0	3.5297E-01	2.2575E-01	2.8322E-01	9.4497E-02	-70.0	2.9970E-02	6.5225E-02	0.
-75.0	3.6033E-01	2.3454E-01	3.0049E-01	1.0647E-01	-75.0	3.7089E-02	7.9097E-02	0.
-80.0	3.6688E-01	2.4249E-01	3.1642E-01	1.1811E-01	-80.0	4.4641E-02	9.3656E-02	0.
-85.0	3.7274E-01	2.4968E-01	3.3113E-01	1.2935E-01	-85.0	5.2521E-02	1.0874E-01	0.
-90.0	3.7803E-01	2.5623E-01	3.4474E-01	1.4018E-01	-90.0	6.0636E-02	1.2419E-01	0.
-95.0	3.8282E-01	2.6223E-01	3.5737E-01	1.5058E-01	-95.0	6.8908E-02	1.3990E-01	0.
-100.0	3.8717E-01	2.6773E-01	3.6910E-01	1.6054E-01	-100.0	7.7270E-02	1.5576E-01	0.
-150.0	4.1582E-01	3.0499E-01	4.5226E-01	2.3927E-01	-150.0	1.5740E-01	3.0889E-01	0.
-200.0	4.3085E-01	3.2527E-01	5.0013E-01	2.9076E-01	-200.0	2.2242E-01	4.3665E-01	0.
-250.0	4.4010E-01	3.3799E-01	5.3108E-01	3.2633E-01	-250.0	2.7274E-01	5.3825E-01	0.
-300.0	4.4637E-01	3.4672E-01	5.5270E-01	3.5221E-01	-300.0	3.1200E-01	6.1920E-01	0.
-350.0	4.5090E-01	3.5307E-01	5.6864E-01	3.7182E-01	-350.0	3.4319E-01	6.8462E-01	0.
-400.0	4.5432E-01	3.5790E-01	5.8088E-01	3.8717E-01	-400.0	3.6847E-01	7.3831E-01	0.
-450.0	4.5700E-01	3.6170E-01	5.9057E-01	3.9951E-01	-450.0	3.8931E-01	7.8306E-01	0.
-500.0	4.5915E-01	3.6476E-01	5.9842E-01	4.0963E-01	-500.0	4.0676E-01	8.2087E-01	0.
-550.0	4.6092E-01	3.6729E-01	6.0492E-01	4.1809E-01	-550.0	4.2157E-01	8.5320E-01	0.
-600.0	4.6240E-01	3.6940E-01	6.1039E-01	4.2526E-01	-600.0	4.3430E-01	8.8114E-01	0.
-650.0	4.6365E-01	3.7120E-01	6.1505E-01	4.3141E-01	-650.0	4.4534E-01	9.0552E-01	0.
-700.0	4.6473E-01	3.7275E-01	6.1908E-01	4.3675E-01	-700.0	4.5502E-01	9.2697E-01	0.
-750.0	4.6567E-01	3.7409E-01	6.2258E-01	4.4142E-01	-750.0	4.6356E-01	9.4598E-01	0.
-800.0	4.6649E-01	3.7527E-01	6.2566E-01	4.4555E-01	-800.0	4.7115E-01	9.6294E-01	0.
-850.0	4.6721E-01	3.7632E-01	6.2840E-01	4.4922E-01	-850.0	4.7795E-01	9.7817E-01	0.
-900.0	4.6786E-01	3.7725E-01	6.3083E-01	4.5250E-01	-900.0	4.8406E-01	9.9192E-01	0.
-950.0	4.6843E-01	3.7808E-01	6.3302E-01	4.5546E-01	-950.0	4.8960E-01	1.0044E+00	0.
-1000.0	4.6895E-01	3.7883E-01	6.3500E-01	4.5814E-01	-1000.0	4.9463E-01	1.0157E+00	0.

* Ratio not computed because either or both windows are extremely broad relative to the lower energy passbands. Consequently, derived spectrum slopes may not be representative of the underlying particle population.

**Negative entries signal the breakdown of approximations used to compute the displayed quantities because small E_0 values, and thus steep spectra, force function arguments to assume large positive or negative values.

Table 5. Positive Spectral Parameter Evaluation of Mean Energies in keV Units for the ATS-6 SSPD Passbands.

E_0	$\Delta E1$	$\Delta E2$	$\Delta E3$	$\Delta E4$	E_0	$\Delta E5$	$\Delta E6$	$\Delta E7$
1.0	10.71	18.56	32.96	55.96	1.0	85.36	135.66	219.16
1.5	16.40	24.34	38.74	61.74	1.5	91.14	141.44	224.94
2.0	19.43	27.47	41.88	64.88	2.0	94.28	144.58	228.08
2.5	21.32	29.52	43.96	66.97	2.5	96.37	146.67	230.17
3.0	22.61	31.00	45.51	68.52	3.0	97.92	148.22	231.72
3.5	23.55	32.14	46.74	69.77	3.5	99.18	149.48	232.98
4.0	24.27	33.04	47.77	70.32	4.0	100.24	150.54	234.04
4.5	24.83	33.77	48.64	71.74	4.5	101.18	151.48	234.98
5.0	25.28	34.38	49.40	72.55	5.0	102.03	152.33	235.83
5.5	25.66	34.89	50.06	73.28	5.5	102.82	153.12	236.62
6.0	25.97	35.32	50.65	73.94	6.0	103.55	153.86	237.36
6.5	26.23	35.70	51.18	74.54	6.5	104.24	154.56	238.06
7.0	26.46	36.03	51.64	75.09	7.0	104.90	155.24	238.74
7.5	26.66	36.32	52.07	75.59	7.5	105.53	155.89	239.39
8.0	26.83	36.57	52.45	76.06	8.0	106.13	156.52	240.02
8.5	26.98	36.80	52.79	76.48	8.5	106.70	157.13	240.64
9.0	27.12	37.00	53.10	76.88	9.0	107.25	157.73	241.24
9.5	27.24	37.18	53.39	77.24	9.5	107.78	158.32	241.83
10.0	27.35	37.35	53.65	77.58	10.0	108.29	158.90	242.42
15.0	28.05	38.41	55.41	79.92	15.0	112.32	164.12	247.94
20.0	28.40	38.95	56.35	81.23	20.0	114.98	168.40	253.21
25.0	28.61	39.28	56.93	82.05	25.0	116.80	171.80	258.37
30.0	28.75	39.50	57.32	82.61	30.0	118.10	174.47	263.47
35.0	28.85	39.66	57.60	83.01	35.0	119.07	176.58	268.55
40.0	28.92	39.77	57.81	83.32	40.0	119.82	178.28	273.60
45.0	28.98	39.86	57.97	83.56	45.0	120.41	179.67	278.65
50.0	29.03	39.94	58.10	83.75	50.0	120.89	180.82	283.68
55.0	29.07	40.00	58.21	83.91	55.0	121.28	181.78	288.71
60.0	29.10	40.05	58.30	84.04	60.0	121.61	182.60	293.74
65.0	29.13	40.09	58.38	84.15	65.0	121.89	183.30	298.76
70.0	29.15	40.13	58.45	84.25	70.0	122.14	183.91	303.77
75.0	29.17	40.16	58.50	84.33	75.0	122.35	184.45	308.79
80.0	29.19	40.19	58.55	84.40	80.0	122.53	184.92	313.80
85.0	29.20	40.21	58.60	84.47	85.0	122.70	185.34	318.81
90.0	29.22	40.23	58.63	84.53	90.0	122.84	185.71	323.82
95.0	29.23	40.25	58.67	84.58	95.0	122.97	186.04	328.83
100.0	29.24	40.27	58.70	84.62	100.0	123.09	186.35	333.84
150.0	29.31	40.38	58.90	84.91	150.0	123.84	188.29	383.89
200.0	29.34	40.43	59.00	85.06	200.0	124.22	189.27	433.91
250.0	29.37	40.47	59.06	85.15	250.0	124.44	189.87	483.85
300.0	29.38	40.49	59.10	85.21	300.0	124.59	190.26	533.45
350.0	29.39	40. 1	59.13	85.25	350.0	124.70	190.55	582.27
400.0	29.40	40.52	59.15	85.28	400.0	124.78	190.76	629.75
450.0	29.40	40.53	59.17	85.30	450.0	124.85	190.92	675.37
500.0	29.41	40.53	59.18	85.32	500.0	124.90	191.06	718.73
550.0	29.41	40.54	59.19	85.34	550.0	124.94	191.17	759.58
600.0	29.41	40.54	59.20	85.35	600.0	124.97	191.26	797.83
650.0	29.42	40.55	59.21	85.36	650.0	125.00	191.33	833.48
700.0	29.42	40.55	59.21	85.37	700.0	125.03	191.40	866.60
750.0	29.42	40.56	59.22	85.38	750.0	125.05	191.45	897.32
800.0	29.42	40.56	59.23	85.39	800.0	125.07	191.50	925.79
850.0	29.43	40.56	59.23	85.40	850.0	125.08	191.55	952.17
900.0	29.43	40.56	59.23	85.40	900.0	125.10	191.59	976.63
950.0	29.43	40.57	59.24	85.41	950.0	125.11	191.62	999.32
1000.0	29.43	40.57	59.24	85.41	1000.0	125.12	191.65	1020.39

Table 5 (Continued)

E_0	ΔH1	ΔH2	ΔH3	ΔH4	E_0	ΔH5	ΔH6	ΔH7	H1P
1.0	172.22	220.07	281.54	257.44	1.0	368.65	515.32	0.00	1.22
1.5	240.60	276.50	324.59	324.62	1.5	423.99	569.94	813.34	2.48
2.0	275.06	304.93	346.33	358.47	2.0	451.93	597.51	839.49	4.37
2.5	295.93	322.27	359.65	378.98	2.5	468.89	614.26	855.38	7.43
3.0	310.01	333.96	368.66	392.82	3.0	480.36	625.59	866.14	12.57
3.5	320.16	342.43	375.24	402.85	3.5	488.70	633.82	873.96	20.87
4.0	327.80	348.87	380.30	410.50	4.0	495.08	640.12	879.96	32.48
4.5	333.74	353.95	384.34	416.56	4.5	500.15	645.13	884.73	45.86
5.0	338.44	358.05	387.67	421.50	5.0	504.30	649.24	888.65	58.96
5.5	342.24	361.43	390.48	425.64	5.5	507.79	652.69	891.94	70.69
6.0	345.36	364.27	392.90	429.17	6.0	510.79	655.65	894.77	80.86
6.5	347.96	366.68	395.02	432.23	6.5	513.40	658.23	897.24	89.63
7.0	350.15	368.76	396.89	434.93	7.0	515.70	660.[illegible]1	899.43	9[illegible].25
7.5	352.01	370.[illegible]6	398.57	437.33	7.5	517.77	662.56	901.40	103.93
8.0	353.62	372.14	400.08	439.50	8.0	519.64	664.41	903.18	109.84
8.5	355.02	373.54	401.46	441.46	8.5	521.35	666.11	904.81	11[illegible].12
9.0	356.25	374.[illegible]8	402.73	443.26	9.0	522.92	667.67	906.32	119.86
9.5	357.33	375.89	403.89	444.92	9.5	524.39	669.12	907.71	124.16
10.0	358.30	376.89	404.96	446.46	10.0	525.75	670.47	909.02	128.08
15.0	364.15	383.20	412.55	457.59	15.0	536.22	680.88	919.15	154.72
20.0	366.90	386.32	416.97	464.[illegible]1	20.0	543.85	688.58	926.68	170.54
25.0	368.50	388.19	419.86	469.24	25.0	550.11	695.19	933.10	182.03
30.0	369.54	389.43	421.89	472.65	30.0	555.40	701.19	938.82	191.36
35.0	370.27	390.31	423.38	475.21	35.0	559.90	706.77	943.96	199.45
40.0	370.81	390.96	424.53	477.19	40.0	563.75	711.97	948.58	206.77
45.0	371.23	391.48	425.44	478.77	45.0	567.04	716.79	952.73	213.57
50.0	371.56	391.88	426.17	480.05	50.0	569.87	721.26	956.45	220.02
55.0	371.83	392.22	426.78	481.11	55.0	572.32	725.37	959.79	226.20
60.0	372.06	392.49	427.29	482.00	60.0	574.45	729.15	962.78	232.18
65.0	372.25	392.73	427.73	482.76	65.0	576.32	732.61	965.47	238.01
70.0	372.41	392.93	428.10	483.41	70.0	577.97	735.79	967.89	243.72
75.0	372.55	393.10	428.42	483.98	75.0	579.42	738.70	970.08	249.34
80.0	372.67	393.26	428.71	484.48	80.0	580.73	741.37	972.07	254.88
85.0	372.78	393.39	428.96	484.92	85.0	581.89	743.82	973.87	260.34
90.0	372.87	393.51	429.19	485.31	90.0	582.94	746.08	975.51	265.75
95.0	372.96	393.61	429.39	485.66	95.0	583.89	748.16	977.02	271.11
100.0	373.03	393.[illegible]1	429.57	485.98	100.0	584.76	750.08	978.40	276.41
150.0	373.51	394.32	430.74	488.00	150.0	590.39	763.26	987.69	326.64
200.0	373.75	394.62	431.32	489.01	200.0	593.29	770.44	992.66	376.30
250.0	373.89	394.80	431.68	489.62	250.0	595.05	774.90	995.74	406.38
300.0	373.99	394.92	431.91	490.02	300.0	596.23	777.93	997.82	439.57
350.0	374.05	395.01	432.08	490.31	350.0	597.08	780.11	999.32	459.14
400.0	374.10	395.07	432.21	490.53	400.0	597.71	781.75	1000.46	478.34
450.0	374.14	395.12	432.31	490.70	450.0	598.21	783.04	1001.34	494.15
500.0	374.18	395.16	432.39	490.84	500.0	598.60	784.07	1002.05	50[illegible].33
550.0	374.20	395.19	432.45	490.95	550.0	598.93	784.92	1002.64	51[illegible].45
600.0	374.22	395.22	432.50	491.04	600.0	599.20	785.62	1003.12	527.94
650.0	374.24	395.24	432.55	491.12	650.0	599.43	786.22	1003.54	536.11
700.0	374.26	395.26	432.59	491.18	700.0	599.62	786.74	1003.89	543.22
750.0	374.27	395.28	432.62	491.24	750.0	599.80	787.18	1004.20	549.45
800.0	374.28	395.30	432.65	491.29	800.0	599.94	787.57	1004.47	554.96
850.0	374.29	395.31	432.68	491.34	850.0	600.08	787.91	1004.71	559.85
900.0	374.30	395.32	432.70	491.38	900.0	600.19	788.22	1004.92	564.23
950.0	374.31	395.33	432.72	491.41	950.0	600.30	788.49	1005.11	56[illegible].18
1000.0	374.32	395.34	432.74	491.44	1000.0	600.39	788.74	1005.28	571.74

Table 6. Negative Spectral Parameter Evaluation of Mean Energies in keV Units for the ATS-6 SSPD Passbands.

E_0	ΔE1	ΔE2	ΔE3	ΔE4	E_0	ΔE5	ΔE6	ΔE7
-1000.0	29.47	40.63	59.36	85.59	-1000.0	125.58	192.85	2013.61
-950.0	29.47	40.63	59.36	85.59	-950.0	125.59	192.88	2034.68
-900.0	29.47	40.64	59.37	85.60	-900.0	125.60	192.91	2057.37
-850.0	29.47	40.64	59.37	85.60	-850.0	125.62	192.95	2081.83
-800.0	29.48	40.64	59.37	85.61	-800.0	125.63	193.00	2108.21
-750.0	29.48	40.64	59.38	85.62	-750.0	125.65	193.05	2136.68
-700.0	29.48	40.65	59.39	85.63	-700.0	125.67	193.10	2167.40
-650.0	29.48	40.65	59.39	85.64	-650.0	125.70	193.17	2200.52
-600.0	29.49	40.66	59.40	85.65	-600.0	125.73	193.24	2236.17
-550.0	29.49	40.66	59.41	85.66	-550.0	125.76	193.33	2274.42
-500.0	29.49	40.67	59.42	85.68	-500.0	125.80	193.44	2315.27
-450.0	29.50	40.67	59.43	85.70	-450.0	125.85	193.58	2358.63
-400.0	29.50	40.68	59.45	85.72	-400.0	125.92	193.74	2404.25
-350.0	29.51	40.69	59.47	85.75	-350.0	126.00	193.95	2451.73
-300.0	29.52	40.71	59.50	85.79	-300.0	126.11	194.24	2500.55
-250.0	29.53	40.73	59.54	85.85	-250.0	126.26	194.63	2550.15
-200.0	29.56	40.77	59.60	85.94	-200.0	126.48	195.23	2600.09
-150.0	29.59	40.82	59.70	86.09	-150.0	126.86	196.21	2650.11
-100.0	29.66	40.93	59.90	86.38	-100.0	127.61	198.15	2700.16
-95.0	29.67	40.95	59.93	86.42	-95.0	127.73	198.46	2705.17
-90.0	29.68	40.97	59.97	86.47	-90.0	127.86	198.79	2710.18
-85.0	29.70	40.99	60.00	86.53	-85.0	128.00	199.16	2715.19
-80.0	29.71	41.01	60.05	86.60	-80.0	128.17	199.58	2720.20
-75.0	29.73	41.04	60.10	86.67	-75.0	128.35	200.05	2725.21
-70.0	29.75	41.07	60.15	86.75	-70.0	128.56	200.59	2730.23
-65.0	29.77	41.11	60.22	86.85	-65.0	128.81	201.20	2735.24
-60.0	29.80	41.15	60.30	86.96	-60.0	129.09	201.90	2740.26
-55.0	29.83	41.20	60.39	87.09	-55.0	129.42	202.72	2745.29
-50.0	29.87	41.26	60.50	87.25	-50.0	129.81	203.68	2750.32
-45.0	29.92	41.34	60.63	87.44	-45.0	130.29	204.83	2755.35
-40.0	29.98	41.43	60.79	87.68	-40.0	130.88	206.22	2760.40
-35.0	30.05	41.54	61.00	87.99	-35.0	131.63	207.92	2765.45
-30.0	30.15	41.70	61.28	88.39	-30.0	132.60	210.03	2770.53
-25.0	30.29	41.92	61.67	88.95	-25.0	133.90	212.70	2775.63
-20.0	30.50	42.25	62.25	89.77	-20.0	135.72	216.10	2780.79
-15.0	30.85	42.79	63.19	91.08	-15.0	138.38	220.38	2786.06
-10.0	31.55	43.65	64.95	93.42	-10.0	142.41	225.60	2791.58
-9.5	31.66	44.02	65.21	93.76	-9.5	142.92	226.18	2792.17
-9.0	31.78	44.20	65.50	94.12	-9.0	143.45	226.77	2792.76
-8.5	31.92	44.40	65.81	94.52	-8.5	144.00	227.37	2793.36
-8.0	32.07	44.63	66.15	94.94	-8.0	144.57	227.98	2793.98
-7.5	32.24	44.88	66.53	95.41	-7.5	145.17	228.61	2794.61
-7.0	32.44	45.17	66.96	95.91	-7.0	145.80	229.26	2795.26
-6.5	32.67	45.50	67.42	96.46	-6.5	146.46	229.94	2795.94
-6.0	32.93	45.88	67.95	97.06	-6.0	147.15	230.64	2796.64
-5.5	33.24	46.31	68.54	97.72	-5.5	147.88	231.38	2797.38
-5.0	33.62	46.82	69.20	98.45	-5.0	148.67	232.17	2798.17
-4.5	34.07	47.43	69.96	99.26	-4.5	149.52	233.02	2798.98
-4.0	34.63	48.16	70.83	100.18	-4.0	150.46	233.96	2494.47
-3.5	35.35	49.06	71.86	101.23	-3.5	151.52	235.02	2183.85
-3.0	36.29	50.20	73.09	102.48	-3.0	152.78	236.28	1870.40
-2.5	37.58	[illegible]	74.64	104.03	-2.5	154.33	237.83	1559.77
-2.0	39.47	53.73	76.72	106.12	-2.0	156.42	239.92	1246.29
-1.5	42.50	56.86	79.86	109.26	-1.5	159.56	243.06	935.60
-1.0	48.23	62.63	85.63	115.03	-1.0	165.33	248.83	622.01

Table 6 (Continued)

E_0	ΔH1	ΔH2	ΔH3	ΔH4	E_0	ΔH5	ΔH6	ΔH7	H1P
-1000.0	374.60	395.70	433.46	492.66	-1000.0	603.97	798.12	1011.81	711.26
-950.0	374.60	395.71	433.48	492.69	-950.0	604.07	798.36	1011.99	714.82
-900.0	374.61	395.72	433.50	492.72	-900.0	604.17	798.64	1012.18	718.77
-850.0	374.62	395.73	433.52	492.76	-850.0	604.29	798.94	1012.40	723.15
-800.0	374.63	395.75	433.55	492.81	-800.0	604.42	799.29	1012.64	72[illegible].04
-750.0	374.64	395.76	433.58	492.86	-750.0	604.57	799.68	1012.91	733.55
-700.0	374.66	395.78	433.61	492.92	-700.0	604.74	800.12	1013.23	739.78
-650.0	374.67	395.80	433.65	492.98	-650.0	604.93	800.63	1013.59	746.89
-600.0	374.69	395.82	433.70	493.06	-600.0	605.16	801.23	1014.01	755.06
-550.0	374.71	395.85	433.75	493.15	-550.0	605.43	801.94	1014.51	764.55
-500.0	374.74	395.88	433.82	493.26	-500.0	605.76	802.78	1015.11	775.67
-450.0	374.77	395.92	433.90	493.40	-450.0	606.15	803.81	1015.84	783.85
-400.0	374.81	395.97	434.00	493.56	-400.0	606.65	805.09	1016.76	804.66
-350.0	374.85	396.04	434.12	493.78	-350.0	607.28	806.74	1017.93	823.86
-300.0	374.92	396.12	434.30	494.07	-300.0	608.13	808.91	1019.50	84[illegible].43
-250.0	375.01	396.24	434.54	494.47	-250.0	609.31	811.93	1021.69	876.62
-200.0	375.15	396.42	434.90	495.07	-200.0	611.06	816.37	1024.97	912.70
-150.0	375.38	396.72	435.50	496.07	-150.0	613.95	823.52	1030.36	956.36
-100.0	375.83	397.32	436.71	498.04	-100.0	619.55	836.02	1040.77	1006.59
-95.0	375.91	397.41	436.90	498.35	-95.0	620.40	838.52	1042.36	1011.89
-90.0	375.98	397.52	437.12	498.70	-90.0	621.35	840.58	1044.10	1017.25
-85.0	376.07	397.63	437.35	499.08	-85.0	622.39	842.82	1046.02	1022.66
-80.0	376.17	397.76	437.62	499.51	-80.0	623.54	845.25	1048.14	1028.12
-75.0	376.28	397.91	437.93	499.99	-75.0	624.83	847.89	1050.50	1033.66
-70.0	376.41	398.08	438.28	500.54	-70.0	626.28	850.77	1053.13	1039.28
-65.0	376.56	398.28	438.68	501.17	-65.0	627.90	853.91	1056.07	1044.99
-60.0	376.73	398.51	439.15	501.90	-60.0	629.75	857.33	1059.39	1050.82
-55.0	376.93	398.78	439.70	502.75	-55.0	631.86	861.05	1063.14	1056.80
-50.0	377.16	399.10	440.36	503.76	-50.0	634.27	865.10	1067.41	1062.98
-45.0	377.45	399.43	441.18	504.98	-45.0	637.06	869.49	1072.28	1069.43
-40.0	377.81	399.98	442.19	506.47	-40.0	640.30	874.22	1077.88	1076.23
-35.0	378.26	400.61	443.49	508.33	-35.0	644.07	879.30	1084.36	1083.55
-30.0	378.86	401.44	445.22	510.71	-30.0	648.48	884.72	1091.96	1091.64
-25.0	379.67	402.60	447.61	513.85	-25.0	653.64	890.50	1101.05	1100.97
-20.0	380.83	404.33	451.11	518.14	-20.0	659.70	896.78	1112.47	1112.46
-15.0	382.61	407.17	456.70	524.30	-15.0	667.01	903.94	1128.28	1128.28
-10.0	385.29	412.70	466.81	533.96	-10.0	676.85	913.25	1154.92	1154.92
-9.5	385.55	413.56	468.28	535.27	-9.5	678.11	914.43	1158.84	1158.84
-9.0	385.77	414.51	469.89	536.67	-9.0	679.46	915.69	1163.14	1163.14
-8.5	385.89	415.[illegible]6	471.64	538.18	-8.5	680.91	917.04	1167.88	1167.88
-8.0	385.85	416.74	473.58	539.83	-8.0	682.48	918.49	1173.16	1173.16
-7.5	385.49	418.06	475.71	541.63	-7.5	684.19	920.07	1179.07	1179.07
-7.0	384.50	419.56	478.10	543.62	-7.0	686.08	921.80	1185.74	118[illegible].74
-6.5	382.11	421.28	480.78	545.85	-6.5	688.18	923.73	1193.36	1193.36
-6.0	375.93	423.27	483.84	548.36	-6.0	690.54	925.89	1202.11	1202.11
-5.5	353.99	425.59	487.36	551.24	-5.5	693.25	928.35	1212.22	1212.22
-5.0	-2837.30**	428.34	491.50	554.59	-5.0	696.39	931.21	1223.80	1223.80
-4.5	460.29	431.67	496.44	558.58	-4.5	700.12	934.58	1236.55	1236.55
-4.0	439.42	435.77	502.49	563.44	-4.0	704.67	938.68	1249.32	1249.32
-3.5	436.97	440.97	510.11	569.54	-3.5	710.36	943.81	1260.21	1260.21
-3.0	440.29	447.78	519.93	577.48	-3.0	717.77	950.47	1267.95	1267.95
-2.5	446.17	457.05	532.22	588.05	-2.5	727.72	959.50	1272.80	1272.80
-2.0	451.78	469.28	544.29	600.80	-2.0	740.31	971.55	1246.23	1246.23
-1.5	455.39	480.40	551.47	610.46	-1.5	750.73	935.47	936.03	936.01
-1.0	457.33	485.40	554.47	614.52	-1.0	624.27	623.79	624.48	624.15

Table 7. ATS-6 Low Energy SSPD Responses in keV Units as a Function of Spectral Parameter.

E_0	ΔE1	ΔE2	ΔE3	ΔE4	E_0	ΔE5	ΔE6	ΔE7
1.0	2.3003E-08	6.5690E-12	4.7763E-18	4.9014E-28	1.0	8.3572E-41	1.1941E-62	6.5082E-99
1.5	2.0841E-06	1.0811E-08	7.3225E-13	1.6050E-19	1.5	4.9352E-28	1.3489E-42	8.9999E-67
2.0	4.1197E-05	8.0821E-07	6.0385E-10	6.1171E-15	2.0	2.5259E-21	3.0193E-32	2.2290E-50
2.5	3.1580E-04	1.3948E-05	4.4085E-08	4.4547E-12	2.5	3.4795E-17	6.3609E-26	1.9865E-40
3.0	1.3654E-03	1.0431E-04	8.6931E-07	4.0716E-10	3.0	2.2579E-14	1.1804E-21	9.6420E-34
3.5	4.0981E-03	4.7116E-04	7.8145E-06	1.0952E-08	3.5	2.4632E-12	1.4128E-18	6.1524E-29
4.0	9.6259E-03	1.5085E-03	4.2242E-05	1.3479E-07	4.0	8.6669E-11	2.9965E-16	2.5746E-25
4.5	1.9037E-02	3.8150E-03	1.6114E-04	9.7604E-07	4.5	1.4213E-09	1.9873E-14	1.7365E-22
5.0	3.3222E-02	6.1343E-03	4.7891E-04	4.8492E-06	5.0	1.3590E-08	5.8107E-13	3.2472E-20
5.5	5.2789E-02	1.5268E-02	1.1828E-03	1.8255E-05	5.5	8.7482E-08	9.3356E-12	2.3810E-18
6.0	7.8055E-02	2.5989E-02	2.5367E-03	5.5684E-05	6.0	4.1767E-07	9.5522E-11	8.6332E-17
6.5	1.0907E-01	4.0974E-02	4.8725E-03	1.4424E-04	6.5	1.5823E-06	6.8976E-10	1.8184E-15
7.0	1.4570E-01	6.0767E-02	8.5722E-03	3.2819E-04	7.0	4.9925E-06	3.7838E-09	2.4970E-14
7.5	1.8764E-01	8.5758E-02	1.4046E-02	6.7257E-04	7.5	1.3598E-05	1.6647E-08	2.4333E-13
8.0	2.3448E-01	1.1619E-01	2.1711E-02	1.2652E-03	8.0	3.2845E-05	6.1183E-08	1.7935E-12
8.5	2.8578E-01	1.5216E-01	3.1967E-02	2.2167E-03	8.5	7.1824E-05	1.9383E-07	1.0499E-11
9.0	3.4105E-01	1.9365E-01	4.5185E-02	3.6589E-03	9.0	1.4452E-04	5.4235E-07	5.0703E-11
9.5	3.9981E-01	2.4056E-01	6.1693E-02	5.7419E-03	9.5	2.7100E-04	1.3665E-06	2.0819E-10
10.0	4.6158E-01	2.9259E-01	8.1766E-02	8.6295E-03	10.0	4.7852E-04	3.1488E-06	7.4454E-10
15.0	1.1621E+00	1.0344E+00	5.0331E-01	1.1901E-01	15.0	1.8829E-02	6.7965E-04	2.6084E-06
20.0	1.8601E+00	1.9710E+00	1.2774E+00	4.5578E-01	20.0	1.2508E-01	1.0835E-02	1.6919E-04
25.0	2.4736E+00	2.9144E+00	2.2506E+00	1.0311E+00	25.0	3.9852E-01	5.9336E-02	2.1799E-03
30.0	2.9948E+00	3.7895E+00	3.2936E+00	1.7851E+00	30.0	8.7195E-01	1.8815E-01	1.2401E-02
35.0	3.4350E+00	4.5755E+00	4.3301E+00	2.6481E+00	35.0	1.5337E+00	4.3399E-01	4.3985E-02
40.0	3.8083E+00	5.2728E+00	5.3211E+00	3.5639E+00	40.0	2.3496E+00	8.1786E-01	1.1577E-01
45.0	4.1273E+00	5.8895E+00	6.2494E+00	4.4935E+00	45.0	3.2801E+00	1.3446E+00	2.4922E-01
50.0	4.4020E+00	6.4356E+00	7.1097E+00	5.4115E+00	50.0	4.2887E+00	2.0070E+00	4.6542E-01
55.0	4.6408E+00	6.9207E+00	7.9027E+00	6.3025E+00	55.0	5.3449E+00	2.7906E+00	7.8302E-01
60.0	4.8499E+00	7.3534E+00	8.6320E+00	7.1576E+00	60.0	6.4247E+00	3.6778E+00	1.2172E+00
65.0	5.0343E+00	7.7410E+00	9.3024E+00	7.9725E+00	65.0	7.5101E+00	4.6500E+00	1.7794E+00
70.0	5.1981E+00	8.0898E+00	9.9191E+00	8.7453E+00	70.0	8.5877E+00	5.6896E+00	2.4775E+00
75.0	5.3445E+00	8.4051E+00	1.0487E+01	9.4763E+00	75.0	9.6480E+00	6.7805E+00	3.3165E+00
80.0	5.4760E+00	8.6912E+00	1.1011E+01	1.0167E+01	80.0	1.0684E+01	7.9086E+00	4.2985E+00
85.0	5.5949E+00	8.9520E+00	1.1496E+01	1.0818E+01	85.0	1.1692E+01	9.0618E+00	5.4238E+00
90.0	5.7027E+00	9.1904E+00	1.1945E+01	1.1432E+01	90.0	1.2669E+01	1.0230E+01	6.6912E+00
95.0	5.8010E+00	9.4093E+00	1.2362E+01	1.2011E+01	95.0	1.3614E+01	1.1405E+01	8.0978E+00
100.0	5.8909E+00	9.6108E+00	1.2749E+01	1.2558E+01	100.0	1.4524E+01	1.2579E+01	9.6404E+00
150.0	6.4948E+00	1.0993E+01	1.5510E+01	1.6659E+01	150.0	2.1919E+01	2.3486E+01	3.1531E+01
200.0	6.8201E+00	1.1759E+01	1.7111E+01	1.9194E+01	200.0	2.6953E+01	3.2170E+01	6.2086E+01
250.0	7.0233E+00	1.2245E+01	1.8152E+01	2.0899E+01	250.0	3.0521E+01	3.8885E+01	9.8057E+01
300.0	7.1622E+00	1.2580E+01	1.8881E+01	2.2120E+01	300.0	3.3163E+01	4.4138E+01	1.3751E+02
350.0	7.2631E+00	1.2825E+01	1.9420E+01	2.3036E+01	350.0	3.5191E+01	4.8327E+01	1.7925E+02
400.0	7.3397E+00	1.3011E+01	1.9835E+01	2.3748E+01	400.0	3.6794E+01	5.1732E+01	2.2249E+02
450.0	7.3999E+00	1.3159E+01	2.0163E+01	2.4318E+01	450.0	3.8092E+01	5.4549E+01	2.6665E+02
500.0	7.4484E+00	1.3278E+01	2.0430E+01	2.4783E+01	500.0	3.9164E+01	5.6914E+01	3.1129E+02
550.0	7.4884E+00	1.3375E+01	2.0651E+01	2.5171E+01	550.0	4.0064E+01	5.8926E+01	3.5604E+02
600.0	7.5218E+00	1.3458E+01	2.0837E+01	2.5498E+01	600.0	4.0829E+01	6.0658E+01	4.0060E+02
650.0	7.5502E+00	1.3529E+01	2.0996E+01	2.5779E+01	650.0	4.1489E+01	6.2164E+01	4.4475E+02
700.0	7.5747E+00	1.3589E+01	2.1133E+01	2.6022E+01	700.0	4.2063E+01	6.3486E+01	4.8828E+02
750.0	7.5959E+00	1.3642E+01	2.1253E+01	2.6234E+01	750.0	4.2567E+01	6.4654E+01	5.3106E+02
800.0	7.6146E+00	1.3688E+01	2.1358E+01	2.6422E+01	800.0	4.3013E+01	6.5634E+01	5.7297E+02
850.0	7.6311E+00	1.3729E+01	2.1451E+01	2.6588E+01	850.0	4.3410E+01	6.6625E+01	6.1392E+02
900.0	7.6458E+00	1.3765E+01	2.1534E+01	2.6737E+01	900.0	4.3766E+01	6.7465E+01	6.5386E+02
950.0	7.6589E+00	1.3798E+01	2.1609E+01	2.6871E+01	950.0	4.4088E+01	6.8225E+01	6.9274E+02
1000.0	7.6708E+00	1.3827E+01	2.1676E+01	2.6992E+01	1000.0	4.4379E+01	6.8916E+01	7.3056E+02

Table 7 (Continued)

E_0	ΔE1	ΔE2	ΔE3	ΔE4
-1.0	3.7782E+17	1.5755E+24	1.5353E+34	9.0041E+46
-1.5	2.3562E+11	3.4967E+15	1.5954E+22	5.1836E+30
-2.0	2.5401E+08	3.4664E+11	3.4244E+16	8.2932E+22
-2.5	5.3875E+06	1.7798E+09	1.7669E+13	2.2624E+18
-3.0	4.5910E+05	5.9608E+07	1.2832E+11	2.3150E+15
-3.5	3.3394E+04	5.6079E+06	4.0671E+09	1.8108E+13
-4.0	2.3902E+04	3.3794E+05	3.1811E+08	4.9630E+11
-4.5	9.2052E+03	2.6198E+05	4.5006E+07	3.1093E+10
-5.0	4.3393E+03	9.1888E+04	9.5878E+06	3.4557E+09
-5.5	2.3629E+03	3.9404E+04	2.7409E+06	5.8076E+08
-6.0	1.4313E+03	1.3599E+04	9.7461E+05	1.3278E+08
-6.5	9.3994E+02	1.0911E+04	4.0922E+05	3.8403E+07
-7.0	6.5726E+02	6.6295E+03	1.9556E+05	1.3345E+07
-7.5	4.8303E+02	4.3175E+03	1.0356E+05	5.3660E+06
-8.0	3.6949E+02	2.9734E+03	5.9580E+04	2.4277E+06
-8.5	2.9204E+02	2.1433E+03	3.6677E+04	1.2097E+06
-9.0	2.3716E+02	1.6045E+03	2.3880E+04	6.5305E+05
-9.5	1.9701E+02	1.2397E+03	1.6295E+04	3.7701E+05
-10.0	1.6682E+02	9.8373E+02	1.1569E+04	2.3037E+05
-15.0	5.8963E+01	2.3210E+02	1.3667E+03	1.0630E+04
-20.0	3.5362E+01	1.1427E+02	4.8048E+02	2.3549E+03
-25.0	2.6094E+01	7.5014E+01	2.5557E+02	9.6356E+02
-30.0	2.1332E+01	5.6766E+01	1.7163E+02	5.3352E+02
-35.0	1.8483E+01	4.6563E+01	1.2827E+02	3.5056E+02
-40.0	1.6605E+01	4.0148E+01	1.0320E+02	2.5617E+02
-45.0	1.5279E+01	3.5733E+01	8.7186E+01	2.0086E+02
-50.0	1.4297E+01	3.2655E+01	7.6208E+01	1.6543E+02
-55.0	1.3542E+01	3.0292E+01	6.8277E+01	1.4118E+02
-60.0	1.2944E+01	2.8450E+01	6.2311E+01	1.2374E+02
-65.0	1.2459E+01	2.6998E+01	5.7679E+01	1.1069E+02
-70.0	1.2058E+01	2.5806E+01	5.3987E+01	1.0062E+02
-75.0	1.1721E+01	2.4816E+01	5.0983E+01	9.2647E+01
-80.0	1.1434E+01	2.3982E+01	4.8493E+01	8.6194E+01
-85.0	1.1187E+01	2.3270E+01	4.6399E+01	8.0879E+01
-90.0	1.0972E+01	2.2655E+01	4.4615E+01	7.6433E+01
-95.0	1.0784E+01	2.2119E+01	4.3078E+01	7.2665E+01
-100.0	1.0617E+01	2.1647E+01	4.1741E+01	6.9435E+01
-150.0	9.6183E+00	1.8890E+01	3.4198E+01	5.2089E+01
-200.0	9.1557E+00	1.7643E+01	3.0961E+01	4.5132E+01
-250.0	8.8891E+00	1.6944E+01	2.9171E+01	4.1417E+01
-300.0	8.7159E+00	1.6490E+01	2.8036E+01	3.9114E+01
-350.0	8.5942E+00	1.6173E+01	2.7253E+01	3.7549E+01
-400.0	8.5041E+00	1.5940E+01	2.6680E+01	3.6416E+01
-450.0	8.4347E+00	1.5761E+01	2.6244E+01	3.5560E+01
-500.0	8.3796E+00	1.5619E+01	2.5899E+01	3.4889E+01
-550.0	8.3348E+00	1.5504E+01	2.5621E+01	3.4350E+01
-600.0	8.2977E+00	1.5409E+01	2.5391E+01	3.3907E+01
-650.0	8.2664E+00	1.5329E+01	2.5199E+01	3.3537E+01
-700.0	8.2396E+00	1.5260E+01	2.5035E+01	3.3222E+01
-750.0	8.2165E+00	1.5201E+01	2.4894E+01	3.2953E+01
-800.0	8.1964E+00	1.5150E+01	2.4771E+01	3.2718E+01
-850.0	8.1786E+00	1.5105E+01	2.4663E+01	3.2513E+01
-900.0	8.1629E+00	1.5065E+01	2.4567E+01	3.2332E+01
-950.0	8.1488E+00	1.5029E+01	2.4482E+01	3.2170E+01
-1000.0	8.1362E+00	1.4997E+01	2.4406E+01	3.2026E+01

E_0	ΔE5	ΔE6	ΔE7
-1.0	6.3016E+68	1.1562+105	4.8880+270
-1.5	1.8984E+45	2.8452E+69	3.5725+271
-2.0	6.9379E+33	9.3977E+51	2.4990+271
-2.5	1.2376E+27	3.9628E+41	6.5226+271
-3.0	4.4284E+22	5.4213E+34	4.9642+271
-3.5	3.1579E+19	7.2514E+29	9.3695+271
-4.0	1.4364E+17	1.6717E+26	7.5669+271
-4.5	2.2270E+15	2.5487E+23	1.1211+271
-5.0	8.1048E+13	1.4504E+21	1.1000+244
-5.5	5.4683E+12	2.1443E+19	8.9000+221
-6.0	5.8494E+11	6.4735E+17	3.5028+203
-6.5	8.9061E+10	3.3798E+16	9.4404+187
-7.0	1.7876E+10	2.7109E+15	4.2959+174
-7.5	4.4719E+09	3.0631E+14	1.1625+163
-8.0	1.3371E+09	4.5700E+13	9.1176+152
-8.5	4.6281E+08	8.5675E+12	1.0932+144
-9.0	1.8090E+08	1.9422E+12	1.2898+136
-9.5	7.6302E+07	5.1655E+11	1.0433+129
-10.0	3.6954E+07	1.5731E+11	4.3335+122
-15.0	3.4146E+05	9.2194E+07	1.8183E+82
-20.0	3.4759E+04	2.4218E+06	1.2908E+62
-25.0	9.0272E+03	2.8364E+05	1.1077E+50
-30.0	3.7132E+03	6.9298E+04	1.0354E+42
-35.0	1.9793E+03	2.5616E+04	1.9518E+36
-40.0	1.2386E+03	1.2227E+04	1.0112E+32
-45.0	8.6178E+02	6.9087E+03	4.7608E+28
-50.0	6.4548E+02	4.3880E+03	1.0491E+26
-55.0	5.0996E+02	3.0326E+03	7.0964E+23
-60.0	4.1926E+02	2.2320E+03	1.1122E+22
-65.0	3.5537E+02	1.7237E+03	3.3250E+20
-70.0	3.0851E+02	1.3823E+03	1.6504E+19
-75.0	2.7299E+02	1.1422E+03	1.2284E+18
-80.0	2.4531E+02	9.6700E+02	1.2704E+17
-85.0	2.2326E+02	8.3514E+02	1.7221E+16
-90.0	2.0536E+02	7.3329E+02	2.9245E+15
-95.0	1.9057E+02	6.5288E+02	6.0029E+14
-100.0	1.7818E+02	5.8817E+02	1.4474E+14
-150.0	1.1659E+02	3.0483E+02	1.9190E+10
-200.0	9.4404E+01	2.1998E+02	2.4057E+08
-250.0	8.3198E+01	1.8102E+02	1.8284E+07
-300.0	7.6485E+01	1.5901E+02	3.3923E+06
-350.0	7.2029E+01	1.4498E+02	1.0427E+06
-400.0	6.8861E+01	1.3528E+02	4.3796E+05
-450.0	6.6495E+01	1.2819E+02	2.2597E+05
-500.0	6.4661E+01	1.2280E+02	1.3442E+05
-550.0	6.3199E+01	1.1856E+02	8.8556E+04
-600.0	6.2006E+01	1.1513E+02	6.2921E+04
-650.0	6.1015E+01	1.1232E+02	4.7344E+04
-700.0	6.0178E+01	1.0996E+02	3.7241E+04
-750.0	5.9462E+01	1.0795E+02	3.0340E+04
-800.0	5.8843E+01	1.0623E+02	2.5421E+04
-850.0	5.8302E+01	1.0474E+02	2.1791E+04
-900.0	5.7825E+01	1.0342E+02	1.9034E+04
-950.0	5.7402E+01	1.0226E+02	1.6888E+04
-1000.0	5.7024E+01	1.0123E+02	1.5181E+04

Table 8. ATS-6 High Energy SSPD Responses in keV Units as a Function of Spectral Parameter.

E_0	ΔH1	ΔH2	ΔH3	ΔH4	E_0	ΔH5	ΔH6	ΔH7	H1P
10.0	1.0771E-15	3.1816E-16	3.5008E-17	4.0591E-19	10.0	1.7539E-22	9.1989E-29	4.1880E-39	2.8986E-06
15.0	1.8283E-10	1.0101E-10	2.8825E-11	1.4084E-12	15.0	8.4338E-15	5.4987E-19	7.0777E-26	3.1935E-04
20.0	8.0887E-08	6.1569E-08	2.8949E-08	3.0567E-09	20.0	6.8133E-11	4.9520E-14	3.3766E-19	4.7827E-03
25.0	3.1974E-06	2.3534E-06	1.9000E-06	3.2560E-07	25.0	1.6153E-08	4.9982E-11	3.6832E-15	2.7827E-02
30.0	3.7431E-05	3.3523E-05	3.1426E-05	7.5189E-06	30.0	6.4324E-07	5.2465E-09	1.8869E-12	9.6509E-02
35.0	2.1788E-04	2.5304E-04	2.3514E-04	7.1821E-05	35.0	9.1522E-06	1.4980E-07	1.6688E-10	2.4457E-01
40.0	8.1838E-04	1.0211E-03	1.0688E-03	3.9342E-04	40.0	6.6060E-05	1.8865E-06	4.8962E-09	5.0498E-01
45.0	2.2938E-03	3.0272E-03	3.4601E-03	1.4641E-03	45.0	3.2730E-04	1.3721E-05	6.8679E-08	9.0511E-01
50.0	5.2358E-03	7.2285E-03	8.9647E-03	4.3067E-03	50.0	1.1576E-03	6.7807E-05	5.7289E-07	1.4650E+00
55.0	1.0292E-02	1.4744E-02	1.9467E-02	1.0319E-02	55.0	3.2695E-03	2.5257E-04	3.2705E-06	2.1976E+00
60.0	1.8082E-02	2.6718E-02	3.7178E-02	2.1404E-02	60.0	7.7944E-03	7.6019E-04	1.4033E-05	3.1097E+00
65.0	2.9137E-02	4.4138E-02	6.4317E-02	3.9726E-02	65.0	1.6298E-02	1.9402E-03	4.8301E-05	4.2031E+00
70.0	4.3867E-02	6.8058E-02	1.0293E-01	6.7550E-02	70.0	3.0732E-02	4.3475E-03	1.3973E-04	5.4764E+00
75.0	6.2547E-02	9.8955E-02	1.5477E-01	1.0708E-01	75.0	5.3326E-02	8.7735E-03	3.5163E-04	6.9254E+00
80.0	8.5321E-02	1.3732E-01	2.2120E-01	1.6030E-01	80.0	8.6472E-02	1.6255E-02	7.8981E-04	8.5441E+00
85.0	1.1222E-01	1.8337E-01	3.0320E-01	2.2894E-01	85.0	1.3259E-01	2.8062E-02	1.6152E-03	1.0326E+01
90.0	1.4319E-01	2.3715E-01	4.0135E-01	3.1435E-01	90.0	1.9401E-01	4.5665E-02	3.0542E-03	1.2262E+01
95.0	1.7808E-01	2.9852E-01	5.1588E-01	4.1756E-01	95.0	2.7290E-01	7.0685E-02	5.4055E-03	1.4346E+01
100.0	2.1671E-01	3.6724E-01	6.4672E-01	5.3922E-01	100.0	3.7116E-01	1.0435E-01	9.0431E-03	1.6569E+01
150.0	7.5204E-01	1.3657E+00	2.7129E+00	2.7337E+00	150.0	2.6310E+00	1.3054E+00	2.3950E-01	4.4829E+01
200.0	1.4018E+00	2.6355E+00	5.5644E+00	6.1708E+00	200.0	7.0552E+00	4.6858E+00	1.2474E+00	7.9932E+01
250.0	2.0372E+00	3.9110E+00	8.5667E+00	1.0066E+01	250.0	1.2781E+01	1.0147E+01	3.3712E+00	1.1778E+02
300.0	2.6140E+00	5.0838E+00	1.1424E+01	1.3953E+01	300.0	1.9011E+01	1.7027E+01	6.5521E+00	1.5590E+02
350.0	3.1236E+00	6.1418E+00	1.4034E+01	1.7621E+01	350.0	2.5258E+01	2.4674E+01	1.0541E+01	1.9289E+02
400.0	3.5700E+00	7.0724E+00	1.6376E+01	2.0995E+01	400.0	3.1265E+01	3.2612E+01	1.5065E+01	2.2804E+02
450.0	3.9610E+00	7.8928E+00	1.8465E+01	2.4060E+01	450.0	3.6914E+01	4.0528E+01	1.9894E+01	2.6101E+02
500.0	4.3044E+00	8.6172E+00	2.0327E+01	2.6832E+01	500.0	4.2164E+01	4.8237E+01	2.4854E+01	2.9173E+02
550.0	4.6075E+00	9.2531E+00	2.1990E+01	2.9337E+01	550.0	4.7014E+01	5.5632E+01	2.9823E+01	3.2024E+02
600.0	4.8762E+00	9.8305E+00	2.3479E+01	3.1603E+01	600.0	5.1481E+01	6.2661E+01	3.4717E+01	3.4666E+02
650.0	5.1159E+00	1.0341E+01	2.4817E+01	3.3657E+01	650.0	5.5592E+01	6.9304E+01	3.9482E+01	3.7113E+02
700.0	5.3307E+00	1.0800E+01	2.6026E+01	3.5523E+01	700.0	5.9378E+01	7.5560E+01	4.4087E+01	3.9380E+02
750.0	5.5241E+00	1.1215E+01	2.7120E+01	3.7224E+01	750.0	6.2868E+01	8.1441E+01	4.8510E+01	4.1484E+02
800.0	5.6991E+00	1.1590E+01	2.8116E+01	3.8780E+01	800.0	6.6091E+01	8.6963E+01	5.2745E+01	4.3437E+02
850.0	5.8582E+00	1.1932E+01	2.9025E+01	4.0206E+01	850.0	6.9072E+01	9.2149E+01	5.6789E+01	4.5254E+02
900.0	6.0032E+00	1.2245E+01	2.9857E+01	4.1519E+01	900.0	7.1835E+01	9.7020E+01	6.0644E+01	4.6948E+02
950.0	6.1361E+00	1.2531E+01	3.0623E+01	4.2729E+01	950.0	7.4401E+01	1.0160E+02	6.4315E+01	4.8528E+02
1000.0	6.2582E+00	1.2794E+01	3.1328E+01	4.3849E+01	1000.0	7.6790E+01	1.0590E+02	6.7809E+01	5.0006E+02
1500.0	7.0899E+00	1.4597E+01	3.6190E+01	5.1655E+01	1500.0	9.3813E+01	1.3779E+02	9.4819E+01	6.0735E+02
2000.0	7.5463E+00	1.5591E+01	3.8897E+01	5.6067E+01	2000.0	1.0370E+02	1.5719E+02	1.1214E+02	6.7128E+02
2500.0	7.8342E+00	1.6220E+01	4.0618E+01	5.8893E+01	2500.0	1.1013E+02	1.7014E+02	1.2402E+02	7.1348E+02
3000.0	8.0322E+00	1.6653E+01	4.1808E+01	6.0856E+01	3000.0	1.1463E+02	1.7936E+02	1.3263E+02	7.4337E+02
3500.0	8.1767E+00	1.6970E+01	4.2679E+01	6.2298E+01	3500.0	1.1796E+02	1.8625E+02	1.3915E+02	7.6564E+02
4000.0	8.2868E+00	1.7211E+01	4.3344E+01	6.3402E+01	4000.0	1.2053E+02	1.9160E+02	1.4425E+02	7.8285E+02
4500.0	8.3734E+00	1.7401E+01	4.3868E+01	6.4274E+01	4500.0	1.2256E+02	1.9586E+02	1.4835E+02	7.9656E+02
5000.0	8.4434E+00	1.7555E+01	4.4293E+01	6.4981E+01	5000.0	1.2421E+02	1.9934E+02	1.5171E+02	8.0772E+02
5500.0	8.5011E+00	1.7682E+01	4.4643E+01	6.5565E+01	5500.0	1.2557E+02	2.0223E+02	1.5451E+02	8.1700E+02
6000.0	8.5494E+00	1.7788E+01	4.4937E+01	6.6055E+01	6000.0	1.2672E+02	2.0466E+02	1.5689E+02	8.2483E+02
6500.0	8.5906E+00	1.7878E+01	4.5187E+01	6.6473E+01	6500.0	1.2771E+02	2.0677E+02	1.5893E+02	8.3152E+02
7000.0	8.6260E+00	1.7956E+01	4.5402E+01	6.6833E+01	7000.0	1.2855E+02	2.0858E+02	1.6070E+02	8.3730E+02
7500.0	8.6568E+00	1.8024E+01	4.5590E+01	6.7147E+01	7500.0	1.2929E+02	2.1016E+02	1.6225E+02	8.4236E+02
8000.0	8.6839E+00	1.8084E+01	4.5755E+01	6.7423E+01	8000.0	1.2994E+02	2.1155E+02	1.6362E+02	8.4681E+02
8500.0	8.7078E+00	1.8136E+01	4.5901E+01	6.7668E+01	8500.0	1.3052E+02	2.1279E+02	1.6484E+02	8.5076E+02
9000.0	8.7292E+00	1.8183E+01	4.6031E+01	6.7885E+01	9000.0	1.3103E+02	2.1389E+02	1.6593E+02	8.5429E+02
9500.0	8.7483E+00	1.8225E+01	4.6148E+01	6.8081E+01	9500.0	1.3150E+02	2.1489E+02	1.6691E+02	8.5746E+02
10000.0	8.7656E+00	1.8263E+01	4.6253E+01	6.8258E+01	10000.0	1.3191E+02	2.1579E+02	1.6780E+02	8.6033E+02

Table 8 (Continued)

E_0	ΔH1	ΔH2	ΔH3	ΔH4	E_0	ΔH5	ΔH6	ΔH7	H1P
-10.0	3.2619E+30	6.5327E+40	1.5212E+50	1.5212E+50	-10.0	3.0552E+17	6.3457E+19	1.8087E+21	1.9046E+24
-15.0	6.0466E+20	4.5392E+27	4.4763E+33	4.4763E+33	-15.0	8.4144E+11	7.3573E+12	3.7247E+14	4.1350E+16
-20.0	9.5148E+15	1.3749E+21	3.4645E+25	3.4647E+25	-20.0	1.4518E+09	9.2008E+09	1.9292E+11	6.9670E+12
-25.0	1.3363E+13	1.8048E+17	5.3987E+20	5.4008E+20	-25.0	3.2395E+07	1.6277E+08	2.1567E+09	3.9987E+10
-30.0	1.7403E+11	4.8544E+14	3.6076E+17	3.6132E+17	-30.0	2.5846E+06	1.1158E+07	1.0997E+08	1.3142E+09
-35.0	8.0160E+09	7.2753E+12	2.0260E+15	2.0343E+15	-35.0	4.2608E+05	1.6529E+06	1.3254E+07	1.1613E+08
-40.0	8.0880E+08	3.1755E+11	4.2625E+13	4.2980E+13	-40.0	1.1044E+05	3.9571E+05	2.7256E+06	1.8964E+07
-45.0	1.3719E+08	2.8181E+10	2.1511E+12	2.1823E+12	-45.0	3.8687E+04	1.3038E+05	7.9914E+05	4.6541E+06
-50.0	3.3406E+07	4.1009E+09	1.9958E+11	2.0410E+11	-50.0	1.6727E+04	5.3677E+04	3.0008E+05	1.5173E+06
-55.0	1.0567E+07	8.5376E+08	2.8770E+10	2.9707E+10	-55.0	8.4276E+03	2.5938E+04	1.3483E+05	6.0769E+05
-60.0	4.0630E+06	2.3225E+08	5.7622E+09	6.0170E+09	-60.0	4.7615E+03	1.4206E+04	6.9283E+04	2.8348E+05
-65.0	1.8144E+06	7.7543E+07	1.4847E+09	1.5699E+09	-65.0	2.9379E+03	8.5240E+03	3.9468E+04	1.4924E+05
-70.0	9.1035E+05	3.0392E+07	4.6596E+08	4.9945E+08	-70.0	1.9425E+03	5.5032E+03	2.4377E+04	8.6073E+04
-75.0	5.0200E+05	1.3535E+07	1.7112E+08	1.8611E+08	-75.0	1.3574E+03	3.7670E+03	1.6061E+04	5.3450E+04
-80.0	2.9840E+05	6.6845E+06	7.1373E+07	7.8825E+07	-80.0	9.9205E+02	2.7041E+03	1.1152E+04	3.5244E+04
-85.0	1.8874E+05	3.5937E+06	3.3050E+07	3.7085E+07	-85.0	7.5236E+02	2.0184E+03	8.0842E+03	2.4414E+04
-90.0	1.2570E+05	2.0731E+06	1.6693E+07	1.9040E+07	-90.0	5.8842E+02	1.5566E+03	6.0747E+03	1.7621E+04
-95.0	8.7431E+04	1.2688E+06	9.0692E+06	1.0519E+07	-95.0	4.7229E+02	1.2337E+03	4.7048E+03	1.3165E+04
-100.0	6.3089E+04	8.1648E+05	5.2419E+06	6.1843E+06	-100.0	3.8752E+02	1.0009E+03	3.7385E+03	1.0129E+04
-150.0	8.0740E+03	5.1297E+04	1.6607E+05	2.3239E+05	-150.0	1.1080E+02	2.6547E+02	8.7371E+02	1.9319E+03
-200.0	2.9090E+03	1.3079E+04	2.9952E+04	4.8834E+04	-200.0	5.9282E+01	1.3759E+02	4.2302E+02	8.4582E+02
-250.0	1.5803E+03	5.7941E+03	1.0765E+04	1.9946E+04	-250.0	4.0740E+01	9.2570E+01	2.7388E+02	5.1570E+02
-300.0	1.0532E+03	3.3755E+03	5.4514E+03	1.1225E+04	-300.0	3.1729E+01	7.1083E+01	2.0502E+02	3.7093E+02
-350.0	7.8853E+02	2.2976E+03	3.3561E+03	7.5390E+03	-350.0	2.6542E+01	5.8854E+01	1.6672E+02	2.9319E+02
-400.0	6.3486E+02	1.7230E+03	2.3337E+03	5.6364E+03	-400.0	2.3216E+01	5.1101E+01	1.4278E+02	2.4530E+02
-450.0	5.3644E+02	1.3779E+03	1.7597E+03	4.5173E+03	-450.0	2.0921E+01	4.5779E+01	1.2657E+02	2.1431E+02
-500.0	4.6886E+02	1.1527E+03	1.4042E+03	3.7965E+03	-500.0	1.9249E+01	4.1923E+01	1.1493E+02	1.9206E+02
-550.0	4.1997E+02	9.9621E+02	1.1676E+03	3.3004E+03	-550.0	1.7981E+01	3.9012E+01	1.0622E+02	1.7559E+02
-600.0	3.8317E+02	8.8227E+02	1.0013E+03	2.9415E+03	-600.0	1.6989E+01	3.6741E+01	9.9461E+01	1.6295E+02
-650.0	3.5457E+02	7.9617E+02	8.7925E+02	2.6715E+03	-650.0	1.6192E+01	3.4923E+01	9.4082E+01	1.5296E+02
-700.0	3.3177E+02	7.2914E+02	7.8659E+02	2.4619E+03	-700.0	1.5539E+01	3.3437E+01	8.9704E+01	1.4490E+02
-750.0	3.1320E+02	6.7566E+02	7.1424E+02	2.2951E+03	-750.0	1.4994E+01	3.2200E+01	8.6075E+01	1.3825E+02
-800.0	2.9782E+02	6.3211E+02	6.5643E+02	2.1595E+03	-800.0	1.4533E+01	3.1155E+01	8.3020E+01	1.3269E+02
-850.0	2.8487E+02	5.9604E+02	6.0934E+02	2.0473E+03	-850.0	1.4139E+01	3.0262E+01	8.0416E+01	1.2797E+02
-900.0	2.7384E+02	5.6572E+02	5.7033E+02	1.9531E+03	-900.0	1.3797E+01	2.9489E+01	7.8169E+01	1.2391E+02
-950.0	2.6434E+02	5.3991E+02	5.3755E+02	1.8729E+03	-950.0	1.3498E+01	2.8814E+01	7.6212E+01	1.2039E+02
-1000.0	2.5607E+02	5.1769E+02	5.0967E+02	1.8039E+03	-1000.0	1.3234E+01	2.8221E+01	7.4493E+01	1.1731E+02
-1500.0	2.0939E+02	3.9687E+02	3.6383E+02	1.4286E+03	-1500.0	1.1681E+01	2.4734E+01	6.4473E+01	9.9550E+01
-2000.0	1.8936E+02	3.4755E+02	3.0744E+02	1.2750E+03	-2000.0	1.0974E+01	2.3155E+01	5.9981E+01	9.1706E+01
-2500.0	1.7828E+02	3.2097E+02	2.7790E+02	1.1920E+03	-2500.0	1.0571E+01	2.2257E+01	5.7438E+01	8.7301E+01
-3000.0	1.7126E+02	3.0440E+02	2.5981E+02	1.1401E+03	-3000.0	1.0310E+01	2.1678E+01	5.5802E+01	8.4482E+01
-3500.0	1.6641E+02	2.9309E+02	2.4762E+02	1.1046E+03	-3500.0	1.0128E+01	2.1273E+01	5.4663E+01	8.2525E+01
-4000.0	1.6287E+02	2.8489E+02	2.3885E+02	1.0789E+03	-4000.0	9.9931E+00	2.0975E+01	5.3824E+01	8.1087E+01
-4500.0	1.6017E+02	2.7867E+02	2.3225E+02	1.0593E+03	-4500.0	9.8897E+00	2.0746E+01	5.3180E+01	7.9986E+01
-5000.0	1.5804E+02	2.7380E+02	2.2709E+02	1.0440E+03	-5000.0	9.8077E+00	2.0564E+01	5.2671E+01	7.9116E+01
-5500.0	1.5632E+02	2.6987E+02	2.2297E+02	1.0316E+03	-5500.0	9.7412E+00	2.0417E+01	5.2257E+01	7.8411E+01
-6000.0	1.5489E+02	2.6664E+02	2.1958E+02	1.0215E+03	-6000.0	9.6860E+00	2.0295E+01	5.1916E+01	7.7828E+01
-6500.0	1.5370E+02	2.6394E+02	2.1676E+02	1.0130E+03	-6500.0	9.6396E+00	2.0192E+01	5.1628E+01	7.7339E+01
-7000.0	1.5269E+02	2.6165E+02	2.1437E+02	1.0057E+03	-7000.0	9.6001E+00	2.0105E+01	5.1383E+01	7.6922E+01
-7500.0	1.5182E+02	2.5968E+02	2.1232E+02	9.9951E+02	-7500.0	9.5659E+00	2.0029E+01	5.1171E+01	7.6562E+01
-8000.0	1.5105E+02	2.5797E+02	2.1054E+02	9.9411E+02	-8000.0	9.5361E+00	1.9963E+01	5.0987E+01	7.6249E+01
-8500.0	1.5039E+02	2.5646E+02	2.0899E+02	9.8937E+02	-8500.0	9.5099E+00	1.9905E+01	5.0825E+01	7.5973E+01
-9000.0	1.4980E+02	2.5514E+02	2.0761E+02	9.8518E+02	-9000.0	9.4866E+00	1.9854E+01	5.0681E+01	7.5729E+01
-9500.0	1.4927E+02	2.5395E+02	2.0639E+02	9.8144E+02	-9500.0	9.4659E+00	1.9808E+01	5.0553E+01	7.5512E+01
-10000.0	1.4880E+02	2.5290E+02	2.0530E+02	9.7810E+02	-10000.0	9.4472E+00	1.9767E+01	5.0438E+01	7.5316E+01

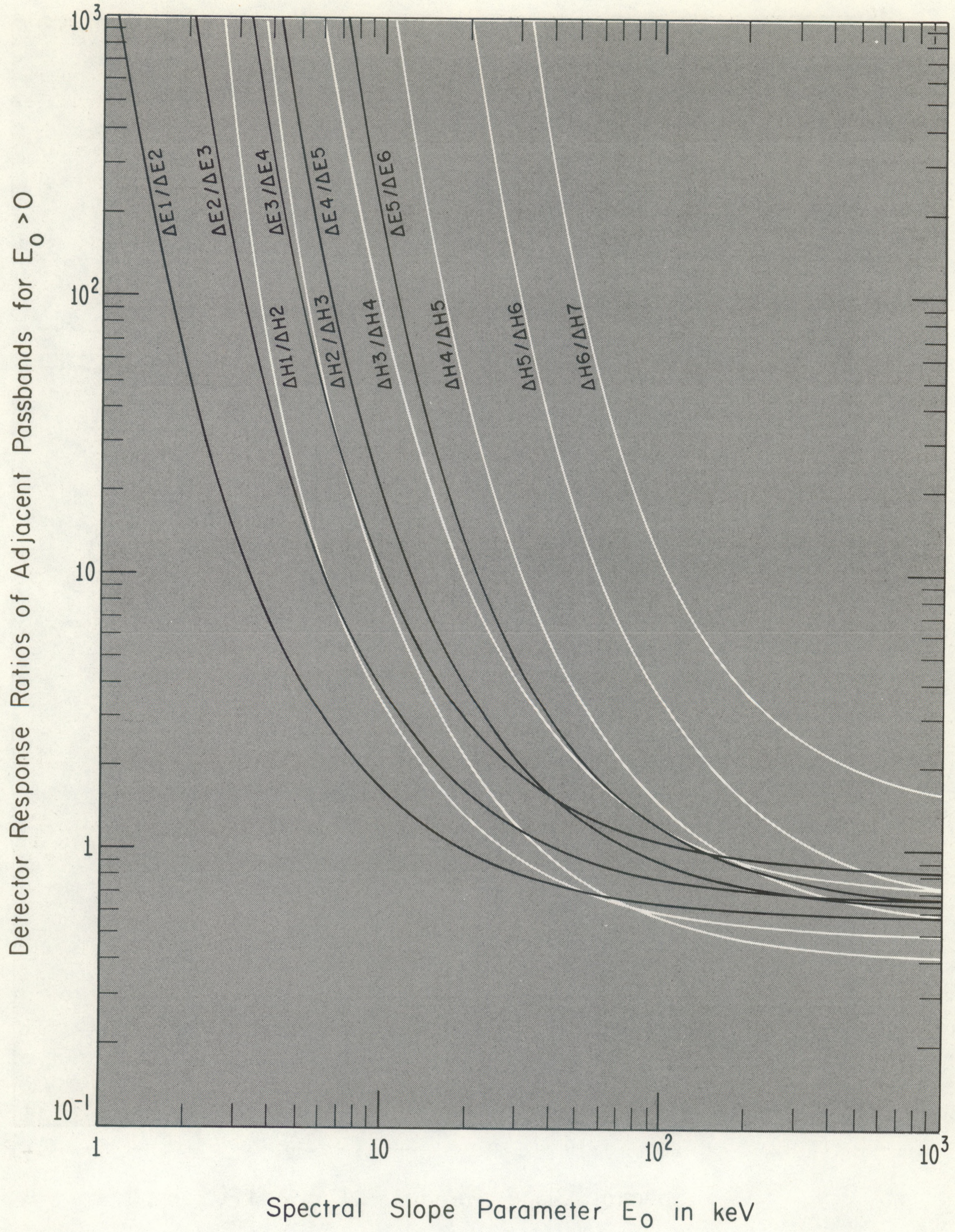

Figure 3. ATS-6 low and high energy SSPD response ratios (always lower window to higher) of adjacent passbands as a function of positive spectral parameter values. Black profiles represent ratios for the lower energy windows ΔE1 through ΔE6; white curves present similar results for the high energy passbands ΔH1 through ΔH7. Table 3 provides a numerical listing of these two families of curves.

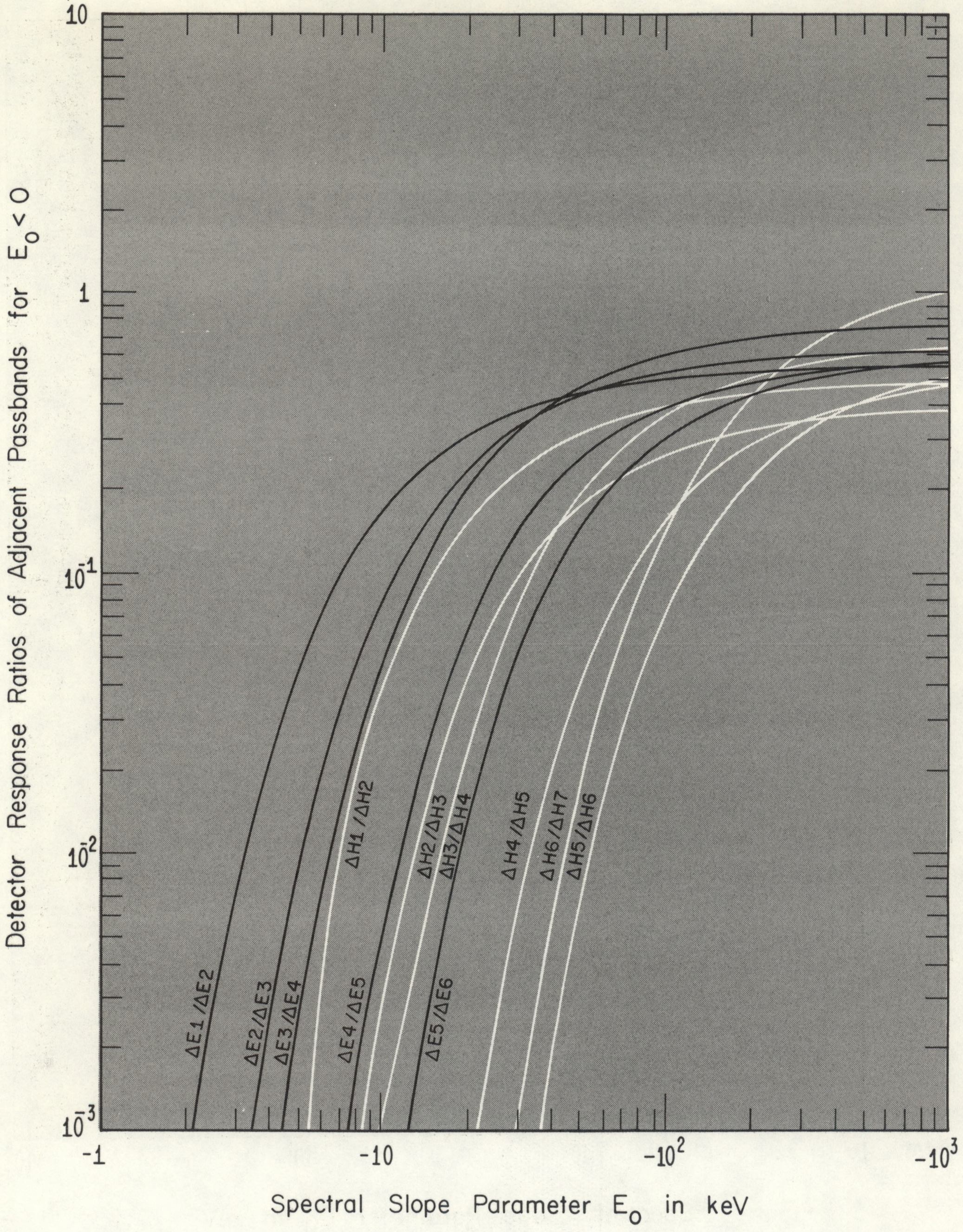

Figure 4. ATS-6 low and high energy SSPD response ratios (always lower window to higher) of adjacent passbands as a function of negative spectral parameter values. Black profiles represent ratios for the low energy windows ΔE1 through ΔE6; white curves present similar results for the high energy passbands ΔH1 through ΔH7. Table 4 provides a numerical listing of these two families of curves.

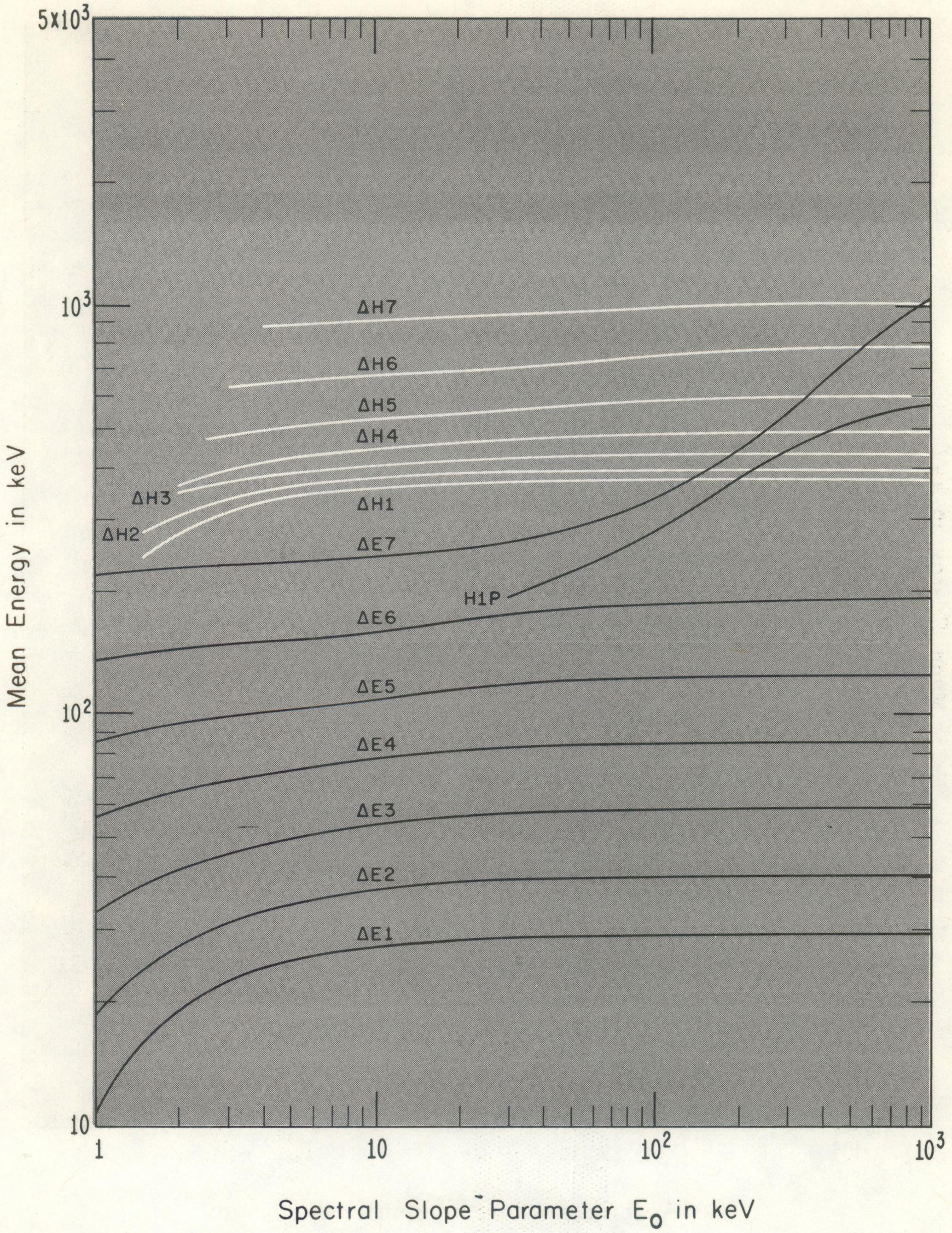

Figure 5. Mean energies of selected ATS-6 low and high energy SSPD passbands as a function of positive spectral parameter values. Table 5 provides a numerical listing of these curves.

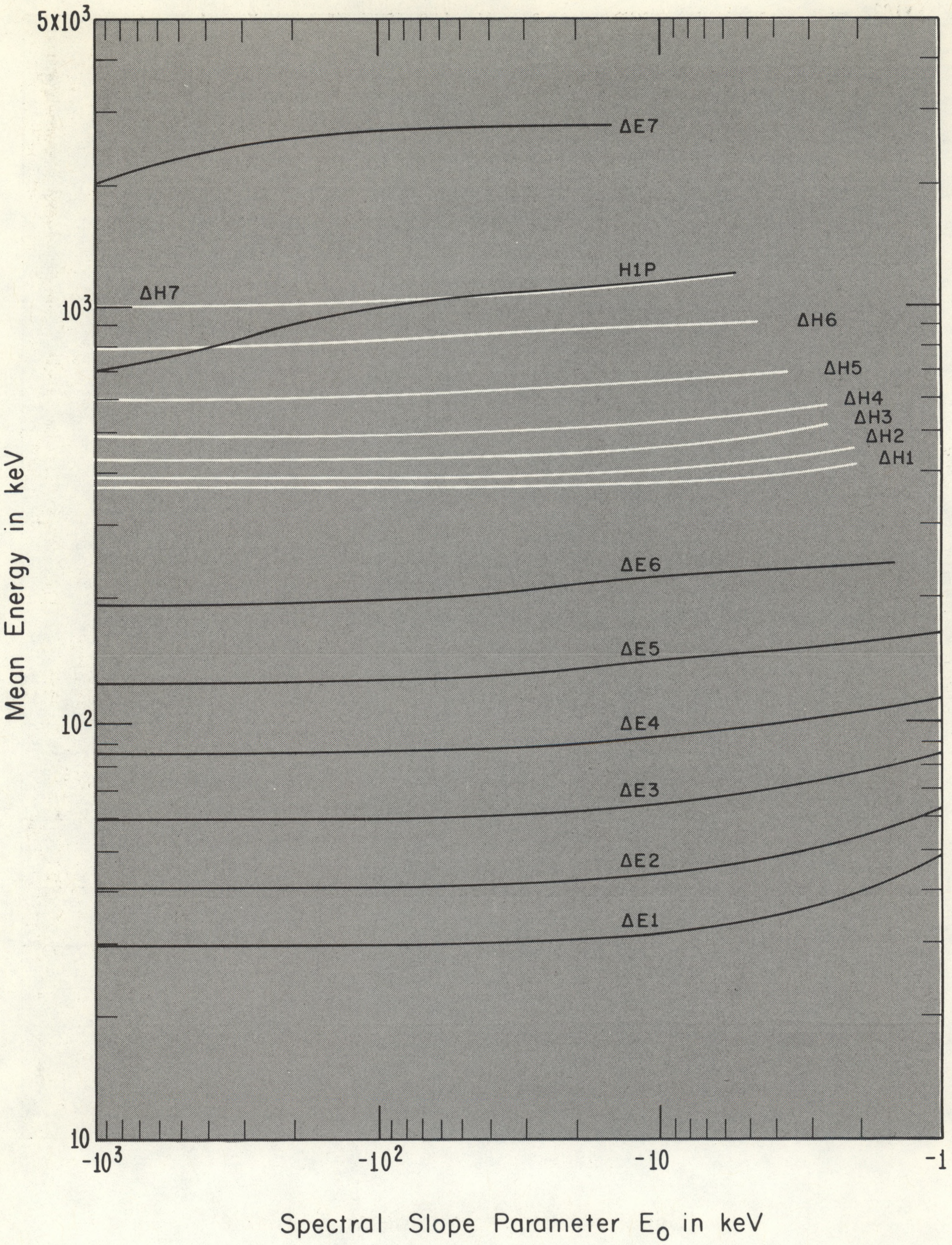

Figure 6. Mean energies of selected ATS-6 low and high energy SSPD passbands as a function of negative spectral parameter values. Table 6 provides a numerical listing of these curves.

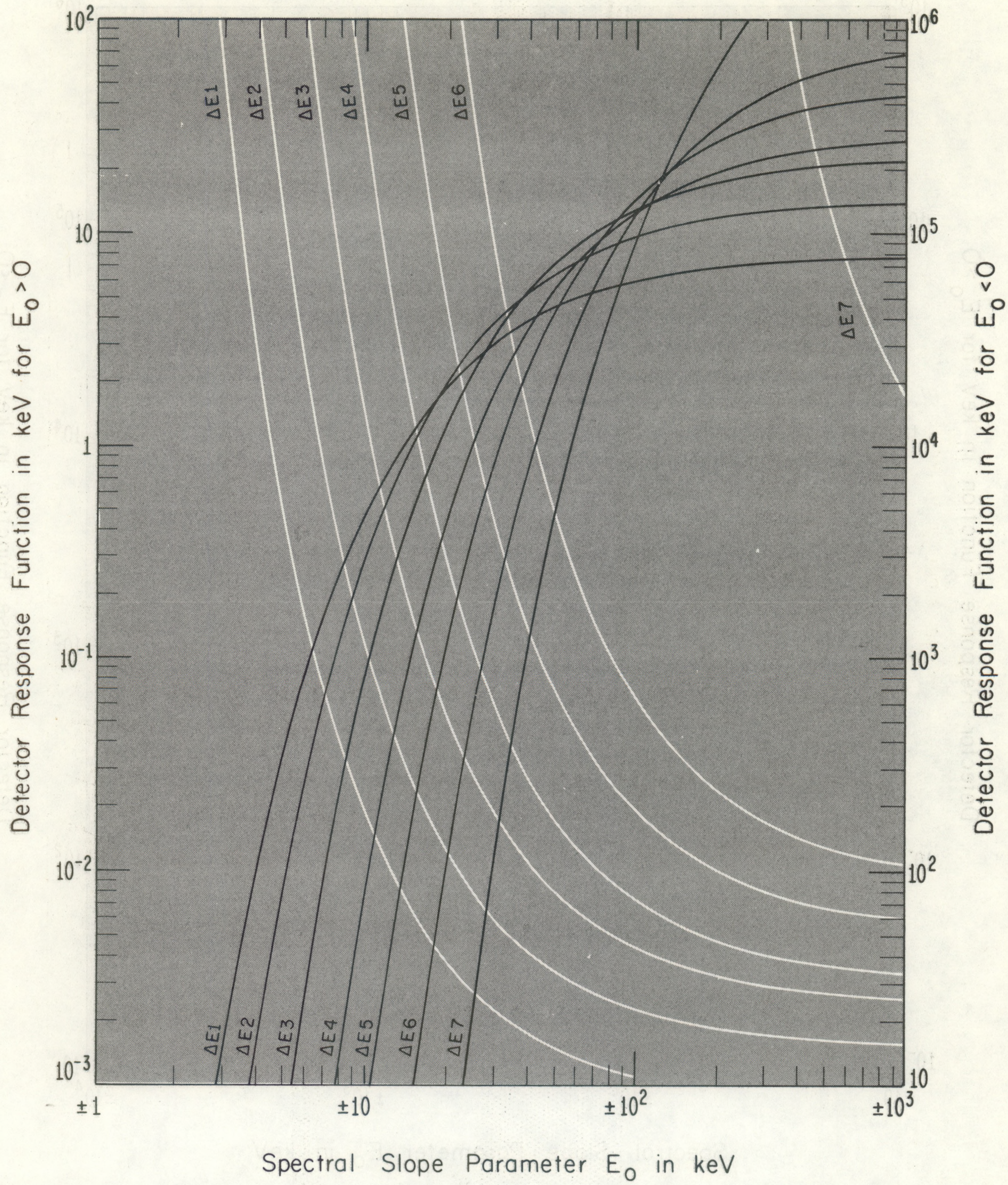

Figure 7. ATS-6 low energy SSPD responses in keV units as a function of spectral parameter. The profiles represent each window's counting rate divided by the product of g, the telescope's geometric factor, and j_0, the y-intercept of an assumed exponential form for the proton differential energy spectrum. Black curves exhibit detector responses over a positive, three-decade range of E_0, and thus display the variation with negative slope spectra. (Read on scale at left.) White curves depict the variation in passband response with positive slope spectra. (Read on scale at right.) Table 7 provides a numerical listing of these two families of curves.

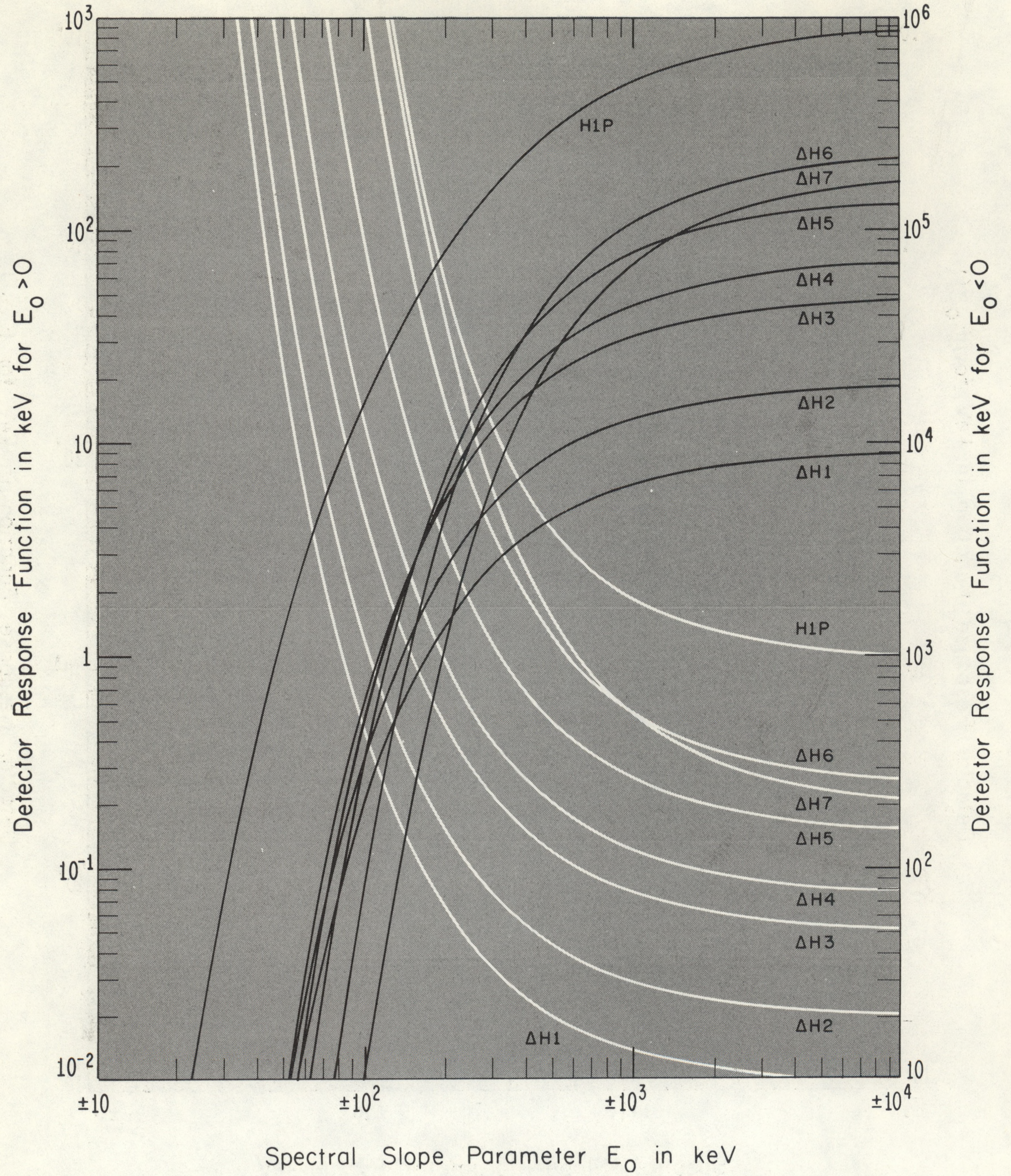

Figure 8. ATS-6 high energy SSPD responses in keV units as a function of spectral parameter. The profiles represent each window's counting rate divided by the product of g, the telescope's geometric factor, and j_0, the y-intercept of an assumed exponential form for the proton differential energy spectrum. Black curves exhibit detector responses over a positive, three-decade range of E_0, and thus display the variation with negative slope spectra. (Read on scale at left.) White curves depict the variation in passband response with positive slope spectra. (Read on scale at right.) Table 8 provides a numerical listing of these two families of curves.

9. VERIFICATION OF RESULTS

An excellent check on the validity of a complicated algebraic expression is to investigate its limit. The limiting value of the mean energy is not difficult to visualize, for when the particle spectrum becomes flat, the spectrum's slope parameter E_0 assumes extremely large positive or negative values. In either case the weighted mean energy converges toward the arithmetic mean of the passband's upper and lower 50% discriminator levels.

Computing the mean energy's asymptotic values requires taking the limits of the detector response function and $(I_3 - I_4)$, a quantity proportional to the mean energy. But since each of these expressions contains many terms, the tedious algebra demanded has been omitted because it is not necessary for appreciating the application of the passband theory to the ATS-6 particle telescope. Suffice it to say that the derived functions do reduce to the values expected of the mean energy, thereby adding some degree of confidence to the correctness of the derived relationships. These results for selected energy passbands are listed in table 2.

The analytical and numerical solutions described in this document serve to fine-tune an energy spectrum profile whenever the passband widths are less than about 100 keV. On the other hand, representative points of wider windows shift considerably with variations in the spectrum's slopes. Counting rates or directional fluxes for each detector channel plotted at their true weighted mean energy rather than at the average of E_n and E_{n+1} insure that jogs in the profile between widely spaced points are real and that the curve's integral will not overestimate the number of charged particles present whenever the slope is negative. Graphing observed counting rates against their passbands' central energies is not incorrect; it simply fails to take advantage of earlier experimenters' results, and more importantly, of all the information contained in the observations.

The white points in figure 9 represent a "corrected" spectrum generated from the theoretical results presented in this document. Along the y axis each point represents an evaluation of the assumed proton spectrum function, $j_0 \exp(-E/E_0)$, at the slope-weighted mean energy of the passband. These functional values are in turn plotted along the x axis at the weighted mean energy of the window. Thus rather than a plot of observed fluxes at their respective arithmetic mean energies as illustrated by the black points in figure 9, a discrete profile of $j_0 \exp(-\langle E \rangle/E_0)$ vs $\langle E \rangle$ has been generated, one more accurately reflecting the changing slope of the underlying continuous spectrum. For broad energy windows and steeply declining spectra the profile when integrated does not tend to overestimate the number of particles present.

10. ACKNOWLEDGMENTS

The authors wish to express thanks to Jacob D. Schroeder for his unusual patience and skill in developing the initial programs associated with this paper's analysis. The expert assistance of Patricia A. Miller, Viola J. Hill, and Linda M. Bath in programming the final form of the results described herein is also gratefully acknowledged.

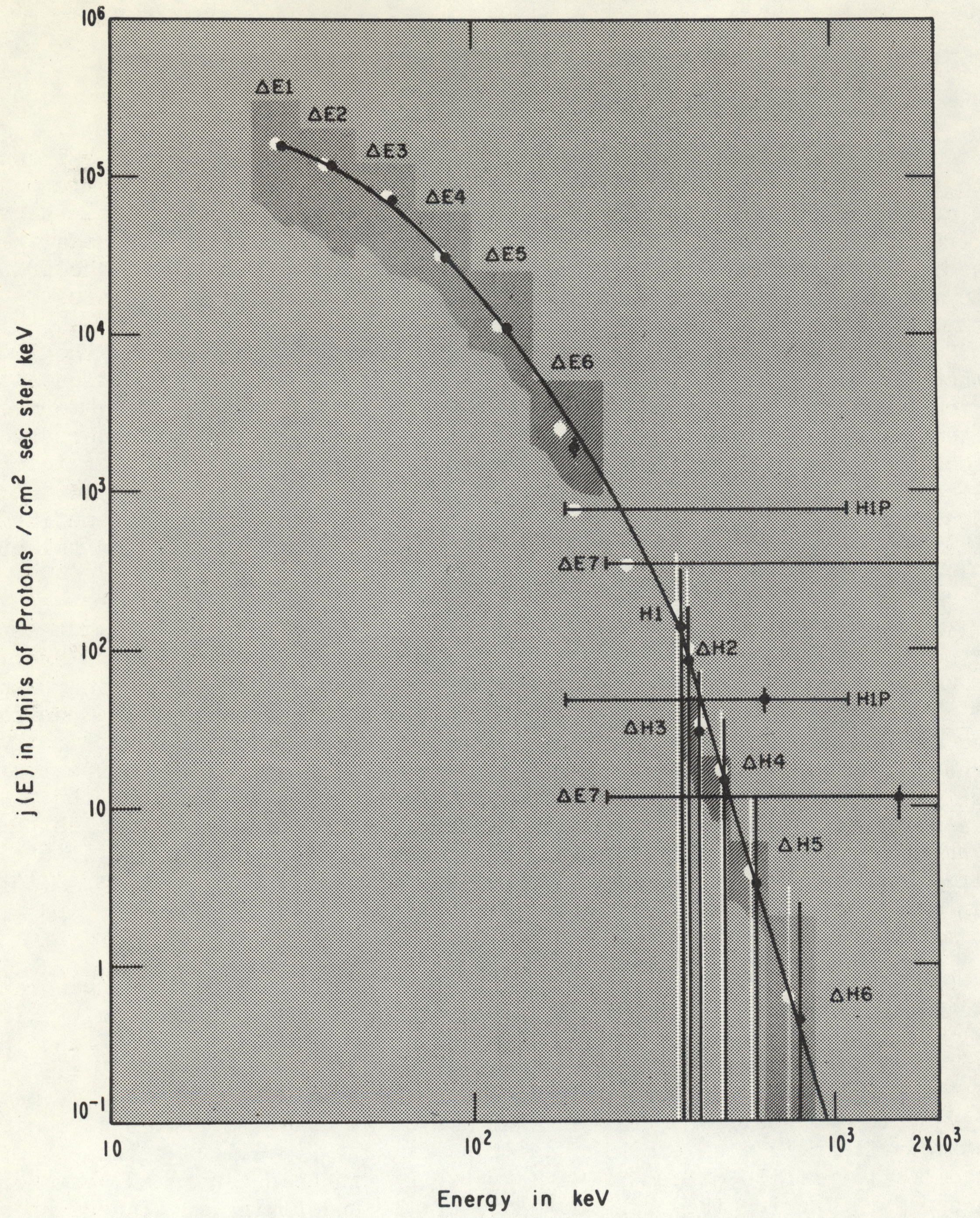

Figure 9. Differential energy proton spectrum. The profile illustrates a quiet-time observation made between 0031 and 0051 UT on 28 July 1974 by the geostationary satellite ATS-6. Black points denote observed flux within each window plotted at the passband's arithmetic mean energy; white points represent an evaluation of $j_0 exp(-\langle E \rangle / E_0)$, the assumed proton spectrum function, graphed against $\langle E \rangle$, the window's slope-weighted mean energy. Density of points and relative passband widths prevented shading the extent in energy of ΔE7, H1P, ΔH1 and ΔH2. The geometric factors used for the low energy B and high energy H telescopes were 7.0 x 10^{-4} and 10^{-3} cm^2 ster.

BIBLIOGRAPHY

Abramowitz, M. and I. A. Stegun, eds. (1964). *Handbook of Mathematical Functions*, Applied Mathematics Series 55, National Bureau of Standards, U. S. Government Printing Office, Washington, D. C.

Fritz, T. A. (1976). S^3 Solid State Proton Experiment. Part I: Design, Operation, and Calibrations, NOAA Tech. Memo. (to be published).

Fritz, T. A. and J. R. Cessna (1975). ATS-6 NOAA Low Energy Proton Experiment, IEEE Transactions on Aerospace and Electronic Systems, Vol. AES-11, Number 6, pp. 1145-54.

Fulks, W. (1965). *Advanced Calculus; An Introduction to Analysis*, Wiley, New York.

Kreyszig, E. (1962). *Advanced Engineering Mathematics*, Wiley, New York.

McKinnon, J. A. and T. A. Fritz (1976). S^3 Solid State Proton Experiment. Part II. Mean Energy of a Finite Energy Passband, NOAA Tech. Memo. ERL SEL-44.

Selby, S. M., ed. (1967). *CRC Standard Mathematical Tables*, Fifteenth Edition, The Chemical Rubber Co., Cleveland, Ohio.

APPENDIX A. DEFINITION OF THE FWHM

Let $\phi_n(E)$ = the cumulative distribution function of the normal probability density function. Then

$$\phi_n(E) = \frac{1}{\sqrt{2\pi}\,\sigma_n} \int_{-\infty}^{E} \exp[-(E'-E_n)^2/2\sigma_n^2]\, dE' \ .$$

Consider initially only the integrand of $\phi_n(E)$ and ask for what values of E' is the function equal to $\frac{1}{2}$ its unit maximum value. If one then denotes this particular value of E' by $E_\pm$, its dependence on E_n and σ_n is readily found. The following four lines outline the straightforward algebra involved.

$$f(E_\pm) = \tfrac{1}{2} = \exp[-(E_\pm - E_n)^2/2\sigma_n^2]$$

$$\ell n(\tfrac{1}{2}) = -(E_\pm - E_n)^2/2\sigma_n^2$$

$$(E_\pm - E_n)^2 = 2\sigma_n^2\, \ell n2$$

$$E_\pm = E_n \pm \sigma_n\sqrt{2\ell n2}$$

The desired value of E' is seen to lie ($\sigma_n\sqrt{2\ell n2}$) units either above or below the mean value, E_n, of the gaussian function. At the same time the interval between these two points along the E' axis defines the full width of the curve at $\frac{1}{2}$ its maximum value. (See figure A.1.) This full width half maximum (FWHM), as it is commonly called, approximately equals $2.35\sigma_n$, a result verified in the next line.

$$\text{FWHM} = (E_+ - E_-) = (E_n + \sigma_n\sqrt{2\ell n2}) - (E_n - \sigma_n\sqrt{2\ell n2}) = 2\sigma_n\sqrt{2\ell n2} \simeq 2.35\sigma_n$$

Although it may not initially seem a fruitful line of inquiry, the following question is a useful one to ask. What values does $\phi_n(E)$ assume for those points at which the integrand equals $\frac{1}{2}$ its maximum value? The answer requires evaluating the following integral:

$$\phi_n(E_\pm) = \frac{1}{\sqrt{2\pi}\,\sigma_n} \int_{-\infty}^{E_\pm} \exp[-(E'-E_n)^2/2\sigma_n^2]\, dE' \ .$$

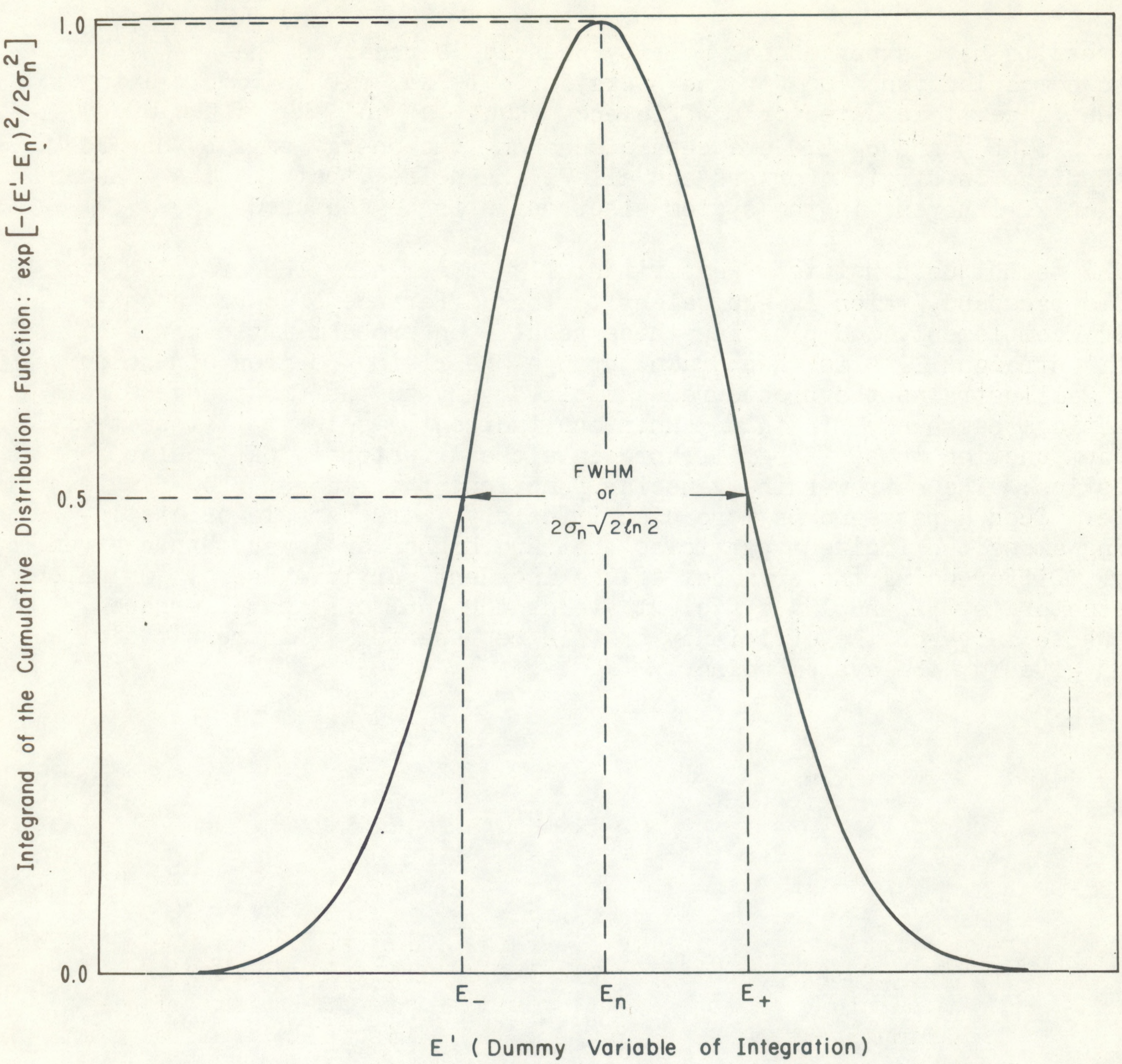

Figure A.1. Definition of the full width at maximum (FWHM) for the gaussian or normal probability density function.

Since ϕ may be transformed into Φ, the finite series approximations given in equations (5) and (6) yield the values shown below.

$$\phi_n(E_-) = \phi_n(E_n - \mathrm{FWHM}/2) = \Phi(-\sqrt{2\ell n 2}) = 0.119 \simeq 12\%$$

$$\phi_n(E_+) = \phi_n(E_n + \mathrm{FWHM}/2) = \Phi(\sqrt{2\ell n 2}) = 0.880 = 88\%$$

These results have experimental utility when it is recalled that $\phi_n(E)$ and its companion function for the backside, $\phi_{n+1}(E)$, may be combined to represent a particle detector's efficiency function, and the values of the integrals $\phi_n(E_-)$ and $\phi_n(E_+)$ are separated along the energy axis by one FWHM. The technique is straightforward and allows the noise, that is, the standard deviation σ, inherent in the system electronics to be measured.

The technique consists of experimentally determining the efficiency of a particle passband, which is equivalent to the difference of $\phi_n(E)$ and its backside complement, and plotting these results on probability paper. A best-fit straight line is then drawn through the rising portion of the curve. Figure 2 illustrates the procedure as applied only to the front edge of a hypothetical passband. In this manner one indirectly selects that best-fit gaussian function whose integral represents the detectors's particular characteristics. The narrower the gaussian function, the steeper the efficiency profile. Such a passband is more discriminatory, more capable of distinguishing among the incident particles that are higher or lower than a given energy. Differencing those values of the incident particle energy for which the detector is 88% and 12% efficient yields the FWHM of the bell-shaped curve whose *integral* the efficiency profile represents. This result divided by 2.35 gives σ, the system noise.

DEFINITIONS OF PRINCIPAL SYMBOLS (continued)

$R_{n,n+1}$	Detector response of the window specified by the 50% transmission energies E_n and E_{n+1}; the integral expression does not include g and j_0 and thus bears energy units rather than counts per second
I_1 and I_2	Partitions of detector response integral ($R_{n,n+1}$) facilitating algebraic manipulations and integrations
E' and E"	Dummy integration variables
α_n and β_n	Groupings of terms within function arguments occurring in the integral expressions I_1 and I_3
α_{n+1} and β_{n+1}	Groupings of terms within function arguments occurring in the integral expressions I_2 and I_4
erf(x)	The error function; integral of the positive half of a standardized gaussian curve multiplied by the normalizing factor $(2/\sqrt{\pi})$
erfc(x)	The complementary error function; integral of the positive tail of a standardized gaussian curve multiplied by the normalizing factor $(2/\sqrt{\pi})$
$r_{n,n+1}$	Ratio of lower window's detector response to that of adjoining upper channel
$\langle E_{n,n+1} \rangle$	Mean energy of a passband delineated by the 50% transmission energies E_n and E_{n+1} and weighted with respect to the energy spectrum's form and the window's efficiency profile
I_3 and I_4	Partitions of integral in numerator of the mean energy expression facilitating algebraic manipulations and integrations
g	Particle telescope geometric factor in cm^2 ster units
E_0	Spectral slope parameter, the negative inverse of which equals the spectrum's slope
j_0	y-intercept of the assumed exponential form of the proton differential energy spectrum
$j_0 \exp(-E/E_0)$	Experimentally verified form of the differential energy spectrum in units of protons/cm^2 sec ster keV